REGISTERED No. M. 3121

OF MICHIGAN
JUN 29 1960
PHYSICS
LIBRARY

PROCEEDINGS

OF THE

INDIAN ACADEMY OF SCIENCES

VOL. LI] SECTION A [No. 4

APRIL 1960

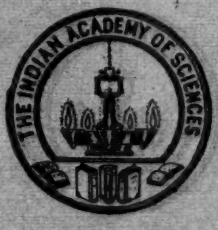

Price Rs. 2 or 3 Sh. *Annual Subscription Rs. 18*

PRINTED AT THE BANGALORE PRESS, BASA[illegible]
SUPERINTENDENT AND PUBLISHER [illegible]
SCIENCES, B[illegible]

POTENTIOMETRIC STUDIES ON THE DISSOCIATION OF GALLIC ACID

By N. A. Ramaiah and R. K. Chaturvedi

(Department of Physical Chemistry, National Sugar Institute, Kanpur)

Received January 26, 1959

(Communicated by Prof. S. N. Gundu Rao, F.A.SC.)

1. Introduction

Gallic acid is one of the important constituents which offer colour to sugarcane juices; and in part contributes to the acid character of the juices. Further gallic acid is employed as an analytical reagent. Thus Neish[1] used gallic acid for precipitation of thorium; Charlot[2] employed the same as a reagent for the ions of the aluminium group; and Datta[3] studied the action of gallic acid on a number of inorganic ions like Cu^{+2}, Hg^{+2}, Al^{+3}. To understand the role of gallic acid in the above process, especially the interaction of the anion of gallic acid and the metallic cations, the knowledge of the dissociation constant k of an apparently primary reaction

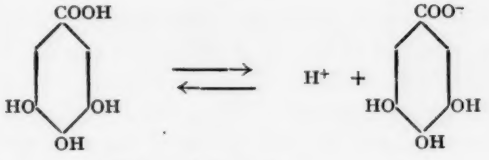

$$HA \leftrightharpoons H^+ + A^- \qquad (1)$$

is of importance. The data on the subject are scanty in the literature. Using conductometric method Ostwald[4] (1889) obtained a value of $3{\cdot}8 \times 10^{-5}$ for the dissociation constant k, while Magnaini[5] (1891) reported that $k = 3{\cdot}4 \times 10^{-5}$; both these results refer to a temperature of 25° C. No data exist in the literature for higher temperatures, which appeared desirable in view of the fact that cane juices are operated in sugar factories at temperatures ranging from 60–80° C. The present communication reports the determination, employing potentiometric method, of the dissociation constants of gallic acid in the range 30–80° C.; these have been employed for calculating the thermodynamic functions such as changes in free energy, entropy, etc., associated with the dissociation of gallic acid.

2. EXPERIMENTAL

Commercial sample (B.D.H.) of gallic acid was purified by recrystallisation in water. Needle-shaped crystals obtained on slow cooling of the saturated solution of the acid were washed with ice-cooled distilled water; this enabled us to get the purest sample with considerable ease. The crystals were later dried at 160° C. The procedure was repeated till the final product gave a constant melting-point (252° C.).

Merck sodium hydroxide was used; no attempt was made to purify this sample. Its solution was standardised in the usual manner by titrating against a solution of known strength of oxalic acid. This last was of Merck " Extra Pure " quality.

It is known that gallic acid gets readily oxidised in presence of alkalies; the titrations had, therefore, to be carried out in an inert atmosphere. For this purpose the solution in the titration flask was deoxygenated at every stage of titration by bubbling purified nitrogen.

The titration was carried out in a vessel immersed in a paraffin oil thermostat maintained at any desired temperature; the constancy of the thermostat was $\pm 0{\cdot}1°$ C.

The hydrogen-ion concentration of the system at every stage of titration was measured by H_2 type pH meter.

3. RESULTS

Figure 1 gives a typical series of results selected out of four sets of data obtained during titration of 60 c.c. of gallic acid solution of known strength against 0·094 N NaOH solution. It was interesting to note that as in other cases employing monocarboxylic acids, a remarkably sharp inflexion could be noticed at the end points over the entire range of temperatures investigated. Prolonged titrations for the apparently possible observation of further one or more inflexions due to interactions with NaOH of the phenolic groups of gallic acid could not be carried out on account of the limitations of our apparatus especially the pH measurements therewith.

4. COMPUTATION OF CLASSICAL DISSOCIATION CONSTANT k

From the data in Fig. 1, the equilibrium concentrations of undissociated acid (HA) and that of anion (A) were computed for different volumes of the titrant added. It follows from the equation

$$k = \frac{[H^+]\,[A^-]}{[HA]} \qquad (2)$$

that value of k could be obtained by plotting corresponding values of pH against log $[HA]\,[A^-]$: the value of pH at log $[HA]/[A] = 0$ gives pk.

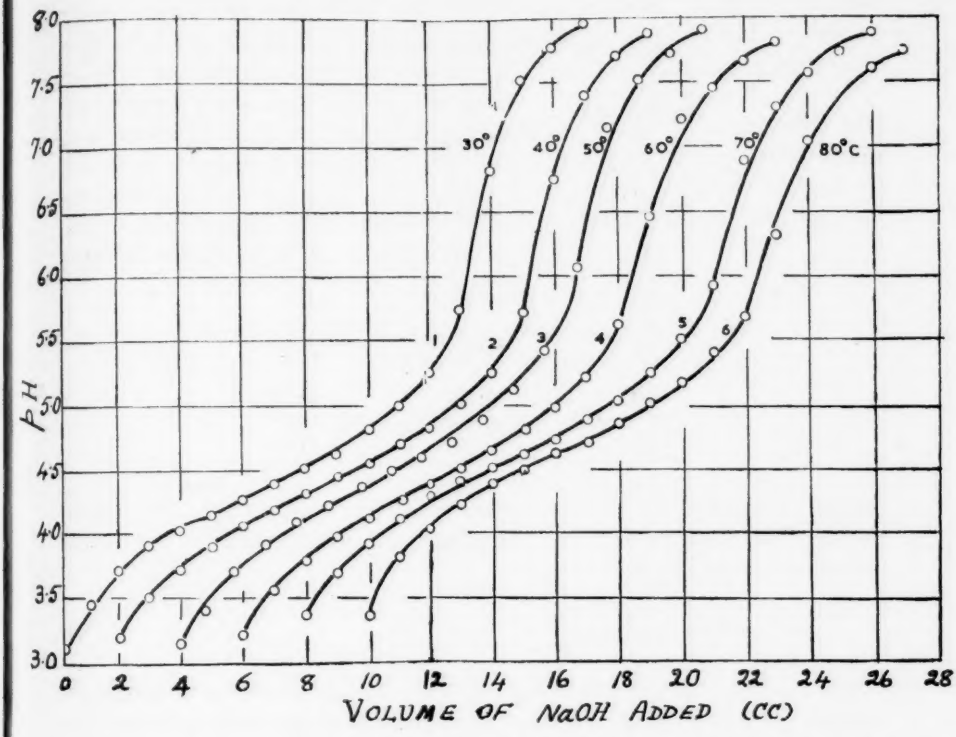

FIG. 1. Curves representing the variation of pH during titration of gallic acid against standard NaOH. The scale on the abscissa is for curve 1; the other curves have been shifted progressively to the right by 2 c.c.

These data are returned in Table I. The data in column 3, Table I, refer to the values of the dissociation constant computed from half neutralisation points on the curves in Fig. 1. It is seen that the values of k obtained by the two methods agree fairly closely. The data in column 2, *i.e.*, the values of k obtained from plots pH *vs.* log [HA]/[A] were, however, employed for further considerations reported hereinafter.

5. CALCULATION OF THERMODYNAMIC DISSOCIATION CONSTANT **K**

Applying the concept of activity coefficients, we get that the thermodynamic dissociation constant **K** of the acid is given by

$$\mathbf{K} = \frac{f_{H^+} \cdot f_{A^-}}{f_{HA}} \cdot \frac{[H^+]\,[A^-]}{[HA]} \qquad (3)$$

TABLE I

Classical dissociation constant of gallic acid

Temperature ° C.	*p*K (From Fig. 1)	*p*K (From Fig. 2)
30	4·38	4·38
40	4·40	4·42
50	4·45	4·45
60	4·46	4·47
70	4·48	4·50
80	4·65	4·68

where f represents the activity coefficients of the constituents. The following modified Debye and Huckel equation[6] can be employed for the computation of the value of f:

$$-\log f_{\pm} = \frac{AZ_i^2\sqrt{\mu}}{1+\sqrt{\mu}} \tag{4}$$

where μ is the ionic strength of the solution. The values of the Debye-Huckel constant **A** employed in the present calculations were due to Bates and coworkers.[7] It is assumed that the activity coefficient of the undissociated molecule is unity. The ionic strengths of the system at different stages of titration were calculated for evaluation of **K**. The values of **K** were obtained from the plots pH *vs.* the ratio of the activities of HA and A^- (*see* Fig. 3). These are given in Table II.

6. THERMODYNAMIC DISSOCIATION CONSTANT OF GALLIC ACID FROM ADDITIVITY PRINCIPLE

Dippy and Williams[8] determined the values of thermodynamic dissociation constants of substituted benzoic acids. The values of **K** for *o*-, *m*- and *p*-hydroxy benzoic acids are given in Table III.[9] It is seen that introduction of a hydroxyl group into the nucleus of the benzoic acid alters the dissociation constant **K** of the acid by a known magnitude depending upon the position of substitution. This is elucidated as follows from the standpoint of the electronic theory of valency.[10, 11] The carboxyl group attached to an aromatic ring is a powerful electron attracting group; it tends to draw

towards itself electrons from *ortho-* and *para*-positions. Consequently the carboxyl group becomes a centre of negative charge while the hydroxyl group acquires an induced positive charge. The dissociation of the proton from the carboxyl group is, therefore, opposed. A hydroxyl group in the *ortho*-position to the carboxyl group, however, tends to form a hydrogen bond with the latter resulting in apparent neutralisation of the induced negative charge on the electronegative group. This renders the proton of the hydroxyl group more tightly bound. The overall effects of the above factors can be summarised as follows[11]:

TABLE II

Thermodynamic dissociation constant of gallic acid

Temperature ° C.	*p*K (From Fig. 3)	*p*K (From Eq. 6)
30	4·46	4·43
40	4·49	4·49
50	4·53	4·54
60	4·56	4·60
70	4·64	4·66
80	4·77	4·72

1. *Hydroxyl group in* ortho-*position.*—Dissociation of COOH group is aided and the dissociation of hydroxyl group is suppressed.

2. *Hydroxyl group in* meta-*position.*—No marked influence is observed.

3. *Hydroxyl group in* para-*position.*—The carboxyl group is rendered less ionisable while the OH group becomes more acidic in character.

Ingold[12] discussed the influence of the substituted hydroxyl group on the dissociation of the carboxyl group of benzoic acid. It is known that it follows a simple addivitity principle in case of *ortho-* and *para*-substituents. Thus the effect of introduction of a hydroxyl group in *ortho*-position to COOH group is to lower the *p*K value by 1·17 units, while the addition of OH in the *para*-position increases *p*K by 0·37 units.

It is of interest to examine the applicability of this additivity principle to compute the thermodynamic dissociation constant K of gallic acid, a

molecule of which contains three hydroxy groups, 2 in *meta*-position and 1 in *para*-position, to —COOH group. This leads to a value of 4·44 for *p*K for gallic acid, in good agreement with observed value of 4·46 at 30° C. (*see* Table III).

7. EFFECT OF TEMPERATURE ON THERMODYNAMIC DISSOCIATION CONSTANT K

The values of **K** obtained at different temperatures in the range 300–360 Å are given in Table III (Fig. 2). It is of interest to note that **K** decreases progressively with rise in temperature. Essentially similar results were

TABLE III

Dissociation constants of substituted benzoic acids

Acid		*p*K	Contribution of the substituted groups
1. Benzoic acid	..	4·17	..
2. O-hydroxy benzoic acid	..	3·30	—1·17
3. *m*-hydroxy benzoic acid	..	4·12	—0·05
4. *p*-hydroxy benzoic acid	..	4·54	+0·37
5. Gallic acid	..	4·44 (4·46)	+0·27

obtained for other carboxylic acids like acetic acid.[13] Detailed examination of the data in Table III shows that the variation of **K** with temperature can be represented by the following equation.[14]

$$-\ln \mathbf{K} = \frac{\mathbf{A}}{\mathbf{T}} + \mathbf{B} + \mathbf{CT}. \qquad (6)$$

The constants **A**, **B** and **C** of equation (6) were computed from the data in Table III employing the method of least squares. These are as follows:

$$\mathbf{A} = 84{\cdot}11$$

$$\mathbf{B} = 5{\cdot}59$$

$$\mathbf{C} = 14{\cdot}29 \times 10^{-3}.$$

It may be noted that equation (6) governs well the variation of **K** with temperature as evidenced by the fact that the values of **K** calculated from

equation (6), agreed closely with those obtained from the experimental data (*cf.* columns 2 and 3, Table II; also Fig. 2).

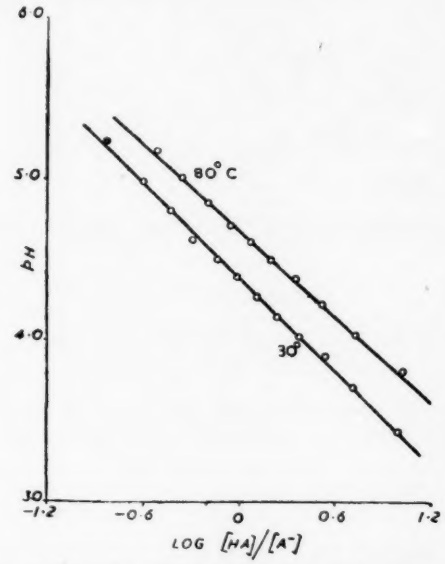

FIG. 2. Computation of classical dissociation constant of gallic acid.

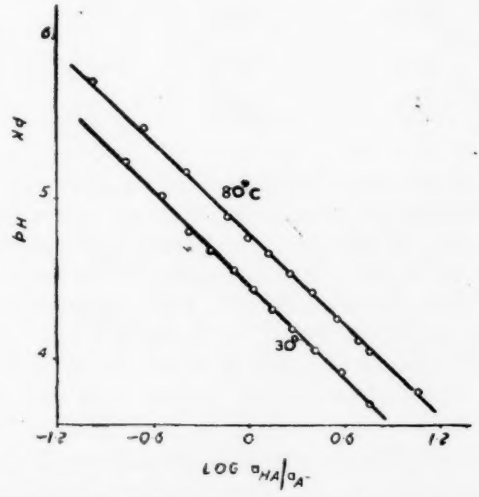

FIG. 3. Computation of thermodynamic dissociation constant of gallic acid.

8. THERMODYNAMIC FUNCTION OF THE DISSOCIATION OF GALLIC ACID

The thermodynamic functions associated with the dissociation of gallic acid were calculated from the constants of equation (6) using the following relationships:

$$\Delta F = R(A - BT - CT^2) \quad (7)$$

$$\Delta H = R(A - CT^2) \quad (8)$$

$$\Delta S = R(- B - 2CT) \quad (9)$$

$$\Delta C_p = R(- 2CT) \quad (10)$$

The values of these functions at different temperatures are returned in Table IV.

TABLE IV

Thermodynamic functions of dissociation of gallic acid

Temperature ° K.	ΔF I.J./mole	ΔH I.J./mole	ΔS I.J./deg./mole	ΔCp I.J./deg./mole
303	25689	−10206	−118·5	−71·9
313	26884	−12335	−120·8	−74·2
323	28105	−13091	−123·2	−76·7
333	29348	−13870	−125·6	−79·1
343	30616	−14672	−127·9	−81·5
353	31906	−15499	−130·3	−83·9

Shorter and Stubbs[15] reviewed the work on the ionisation of substituted benzoic acids. These authors showed that the change in free energy of ionisation is altered by each substituent by a characteristic amount. The effect on the free energy of ionisation of two substituents in the same nucleus is roughly the sum of their individual effects. Thus, substitution of a hydroxyl group in the *para*-position was found to change ΔF by + 500 cals./mole, while ΔF for *meta*-substituted acid differed from that of the benzoic acid by − 120 cals./mole. These considerations suggest that ΔF for gallic acid should have a value of 24·93 kilointernational joules/mole at 25° C. in accord with a value of 25·689 kilointernational joules/mole at 30° C. obtained in the present work.

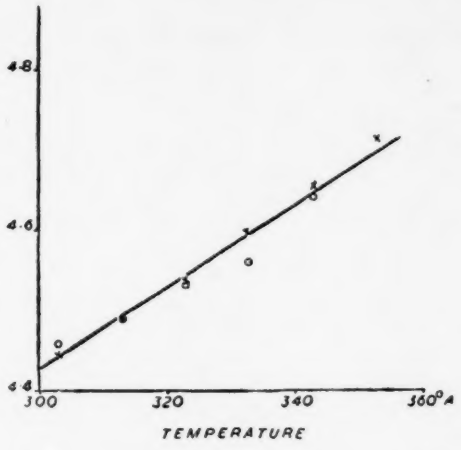

FIG. 4. Variation of p*k* with temperature of the system. O, observed; *x*, calculated.

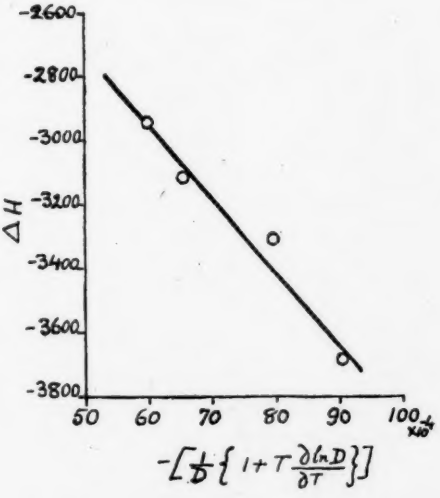

FIG. 5. Linear variation of ΔH with $\frac{1}{D}\left[1+T\frac{\partial \ln D}{\partial T}\right]$

9. IONIC RADIUS OF GALLIC ACID ANION

Baughan[16,17] on the basis of the theoretical suggestions made by Gurney derived the equation for ΔH in terms of the heat of ionization (ΔH_x), dielectric constant **D**, etc.

$$\Delta H = \Delta H_x + C\left[\frac{1}{D}\left((1 + T\frac{\partial ln D}{\partial T}\right)\right]. \tag{11}$$

Here ΔH_x may be regarded either as the heat of ionisation in a medium of infinite dielectric constant where no electric work would be involved, or as the heat effect if there were no separation of the electrical charges in the dissociation process.[18] Equation (11) requires that ΔH should be linearly variant with

$$\left[\frac{1}{D}\left(1 + T\frac{\partial ln D}{\partial T}\right)\right].$$

For evaluation of this expression, Wyman's[19, 20] data on dielectric constants were employed. It is instructive to note from the data in Fig. 4 that the plot of ΔH in cals./mole *vs.*

$$\left[\frac{1}{D}\left(1 + T\frac{\partial ln D}{\partial T}\right)\right]$$

was sensibly linear in accord with equation (11). The slope of the plot in Fig. 4 gives the value of **C** of equation (11). Born[21] observes that **C** refers to the work involved in creating the electrical field around the anion and is given by

$$C = \frac{N\epsilon^2}{2}\left(\frac{1}{r^+} + \frac{1}{r^-}\right) \tag{12}$$

where ϵ is the elementary charge, **N** Avogadro number and r^+ and r^- are the radii of hydronium ion and the gallic acid anion. Using a value of $6{\cdot}02 \times 10^{23}$ for **N**, $4{\cdot}8 \times 10^{-10}$ for ϵ and 0·74 Å for the *ionic radius* of hydronium ion,[22] we obtain a value of 0·78 Å as the radius of the gallic acid anion. It is instructive to compare this value with the *ionic radii* of the anions of acetic acid and formic acid, which are 0·77 and 0·68 Å respectively.[23]

9. SUMMARY

Dissociation of gallic acid at different temperatures in the range 300–380 Å was investigated using glass and calomel electrodes. Applying modified Debye-Huckel equation the thermodynamic dissociation constant **K** was calculated. The variation of **K** with temperature **T** appeared to follow:—

$$-ln K = \frac{A}{T} + B + CT$$

where the constants **A**, **B** and **C** for gallic acid were 84·11, 5·59 and 14·29 $\times 10^{-3}$ respectively. From these, the thermodynamic functions ΔF, ΔH, ΔS and ΔCp were computed. The effect of substitution of three hydroxyl groups in the nucleus of benzoic acid on *p*K and ΔF was discussed. The radius of the anion of gallic acid was computed from the calculated values of ΔH; it corresponded to 0·78 Å.

10. Acknowledgement

Authors' grateful thanks are due to Professor S. N. Gundu Rao, B.Sc., A.H.B.T.I., F.R.I.C., F.A.Sc., Director, National Sugar Institute, for his kind interest in the work, to Ministry of Education for a Fellowship to one of us (R. K. C.) and the U.P. Scientific Research Committee for a contingency Grant. Authors acknowledge with thanks the assistance of Dr. S. L. Gupta, Birla College, Pilani, in the experimental work.

11. References

1. Neish .. *Chemical News*, 1904, **90**, 196.
2. Charlot .. *Anal. Chem. Acta*, 1948, **1**, 218.
3. Datta .. *J. Ind. Chem. Soc.*, 1955, **32**, 687.
4. Ostwald .. *Zeit. F. Physik Chemie*, 1889, **3**, 369.
5. Magnaini .. *Gaz. Chemica Italiana*, 1891, **21**, 215; *cf.*, *Int. Critical Tables*, VI, 230.
6. Guggenheim and Schindler J. *Physic. Chem.*, 1934, **38**, 539.
7. Manov, Bates, Hamer and Acree *J. Am. Chem. Soc.*, 1943, **65**, 1765.
8. Dippy and Williams .. *J. Chem. Soc.*, 1934, 1888.
9. Feiser and Feiser .. *Organic Chemistry*, 2nd Edition, D. C. Heath & Co., Boston, p. 1950, 695.
10. Remick .. *Electronic Interpretations of Organic Chemistry*, 2nd Edition, John Wiley & Sons, Inc., 1949, pp. 64–65.
11. Mathews and Welch .. *J. Appl. Chem.*, 1958, **8** (2), 713.
12. Ingold .. *Structure and Mechanism in Organic Chemistry*, G. Bell and Co., Ltd., London, 1953, p. 738.
13. Noyes .. *J. Amer. Chem. Soc.*, 1908, **30**, 935.
14. Harned and Robinson .. *Trans. Faraday Soc.*, 1940, **36**, 973.
15. Shorter and Stubbs .. *J. Chem. Soc.*, 1949, 1180.
16. Baughan .. *J. Chem. Phys.*, 1931, **7**, 951.
17. Harned and Owen .. *Physical Chemistry of Electrolytic Solutions*, Reinhold Publishing Corporation, New York, 2nd Edition, 1950, p. 530.

18. La Mer and Brescia .. *J. Amer. Chem. Soc.*, 1940, **62**, 617.
19. Wyman and Ingalles .. *Ibid.*, 1938, **60**, 1182.
20. Robinson and Stokes .. *Electrolyte Solutions*, Butterworth's Scientific Publications, London, 1955, p. 447.
21. Born .. *Z. Physik*, 1920, **1**, 45.
22. Kapustinsky .. *Acta Physicochem.*, 1941, **14**, 503.
23. *Cf.* Ref., 17, 0·532.

STUDY OF SOLAR FLARES USING COSMIC RADIO NOISE ON 25 Mc./s. AT AHMEDABAD (23°02′ N., 72°38′ E.)

By R. V. Bhonsle

(*Physical Research Laboratory, Ahmedabad*)

Received January 4, 1960

(Communicated by Dr. K. R. Ramanathan, F.A.SC.)

Abstract

The paper describes observations made at Ahmedabad of sudden cosmic noise absorptions (SCNA's) on 25 Mc./s. associated with solar flares. The frequency distributions of solar flare attenuations, their times of growth and duration, etc., have been determined and the results are compared with similar observations made by other workers. It has been found that SCNA's of 25 Mc./s. recorded at Ahmedabad in 1956–58 have been markedly larger in size and duration than those observed in Australia on 18·3 Mc./s. in 1950–51.

1. Introduction

It is now generally known[1–2] that the measurement of cosmic radio noise provides an effective means of studying the attenuation of radio waves passing through the whole ionosphere. The equipment for measuring the level of cosmic radio noise usually consists of a directional aerial pointed towards the zenith and connected to a stable communications receiver, its output being amplified and recorded on a recording milliammeter. A diode noise generator is used for calibration. The D and F_2-regions are the principal attenuating regions. While the absorption in the D-region is mainly a function of the sun's zenith distance, the attenuation in the F_2-region depends on the value of f_0 F_2, the amount of F-scatter and the electron distribution above the maximum of F_2. Though under normal conditions, the diurnal variation of the total ionospheric attenuation is fairly smooth, sudden and rapid increases in the total attenuation followed by gradual recoveries are sometimes observed. They usually occur during the daytime and are associated with solar flares. The course of a solar flare can be followed by measuring the width of the H_α line in the spectrum of the flare, *i.e.*, the wavelength

interval over which the flare appears brighter than the background. The principal effect of the flare-radiations on the ionosphere is to enhance the electron concentration in the D-region. This causes short wave radio fade-outs, sudden cosmic noise absorptions (SCNA) and sudden phase anomalies in low frequency wave propagation (SPA). Shain and Mitra[3] have analysed the SCNA's observed on 18·3 Mc./s. in Australia and compared the results with the observations of SPA's on 16 Kc./s. observed by Bracewell and Straker[4] in England. They showed that an SCNA of maximum intensity of 1 db was equivalent to an SPA of size 200°. Ramanathan *et al.*[5] reported on the characteristics of two SCNA'S which occurred on 23rd February 1956 and 10th March 1956; the former was of exceptional intensity and caused cosmic ray increases near the geomagnetic equator (V. Sarabhai *et al.*[6]). Since then, about 80 SCNA's have been recorded at the Physical Research Laboratory, Ahmedabad (23° 02′ N., 72° 38′ E.), India. The present paper gives an analysis of the results. The list of SCNA'S is given in Table IV.

2. An Example of an SCNA and Associated Ionospheric Fade-Out

Figure 1 (*a*) shows the record of an SCNA which occurred on the 27th January 1957 at 1245 hr. 75° EMT. It was characterised by a sudden reduction in the intensity of cosmic radio noise on 25 Mc./s. at the time of a solar flare. The intensity of cosmic radio noise continuously decreased till a minimum was recorded at 1250 hr. The maximum absorption was about 6·5 db. Thereafter, a gradual recovery started and the noise level was normal by about 1330 hr. This is the usual pattern of SCNA's, but the rates of growth and decay vary widely from one SCNA to another. In general, the growth of an SCNA is rapid and the recovery slow. Figure 1 (*b*) shows a sequence of three records of ionospheric pulse reflections taken before, during and after the solar flare associated with the SCNA described above. The first record at 12 hr. shows that the reflections were normal. The second at 13 hr. shows an absence of reflections up to 14 Mc./s. This represents a partial ionospheric fade-out caused by the solar flare. The third record at 14 hr. shows that normal ionospheric reflections had again been established. Intense solar flares usually produce complete radio fade-outs which disrupt wireless communication on short waves for sometime. Cosmic noise-fade-out on 25 Mc./s. is usually of a partial nature and during most solar flares, measurable intensity of cosmic noise can be observed. There have been a few instances when there was almost complete fade-out on 25 Mc./s., but such occasions are rare. Since cosmic noise records are continuous, it is possible to study the progress of solar flares even when the sun is obscured owing to cloud.

3. Classification of SCNA's

As seen from the cosmic noise records at Ahmedabad, it has been found to be convenient to classify SCNA's into four types; examples of them are shown in Fig. 2, where the excess absorption due to flare expressed in db is plotted against time. An SCNA of type A is characterised by a sudden

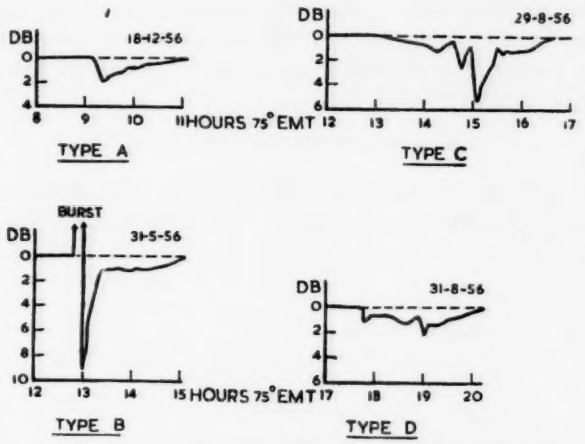

Fig. 2. Four types of SCNA's. Type A, Type B, Type C and Type D.

increase in absorption, an SCNA of type B is accompanied by bursts of solar radio noise, type C is associated with multiple or extended solar flares, and an SCNA is said to be of type D when it is observable at a time when the sun is low in the sky. The SCNA's were classified on this broad qualitative basis, irrespective of the maximum intensity, or in other words, of the maximum absorption produced by the ionosphere. SCNA's of type B are the most common. For a quantitative study of SCNA's, one has to examine the records in detail by noting the times of start, and growth, their duration and "size". The maximum absorption during an SCNA expressed in db is termed the "size" of an SCNA. Absorption at a given time during an SCNA is the ratio, expressed in db, of the observed power to the power that would have been received at that time, had there been no SCNA. While the times of start and growth of SCNA's can be read with an accuracy of $\pm$ 1 min., the duration cannot be estimated with equal precision. The slow rate of recovery towards the end of an SCNA is mainly responsible for this. However the time taken by an SCNA to recover to half the size can be measured with fair accuracy.

4. INTENSITY OF SOLAR FLARE AND SIZE OF SCNA

Bracewell and Straker[4], and Shain and Mitra[3] from their studies of SPA's of 16 Kc./s. and SCNA's of 18·3 Mc./s., conclude that in general, solar flares of classes 3, 2 and 1 were associated with intense, moderate and small SPA's and SCNA's. It has been observed from our studies of SCNA's of 25 Mc./s. that solar flares of class 3 or 3^+ are usually associated with SCNA's of large size but since the size of an SCNA depends not only on the intensity of the flare as determined optically but also on the sun's zenith distance at the time of the flare, a solar flare of class 1 may cause an SCNA of size greater than that caused by a class 2 solar flare.

5. CHARACTERISTICS OF SCNA's

(*a*) *Size*.—Figure 3 represents the frequency distribution of the sizes of SCNA's of 25 Mc./s. at Ahmedabad. It is clearly seen that the mode of

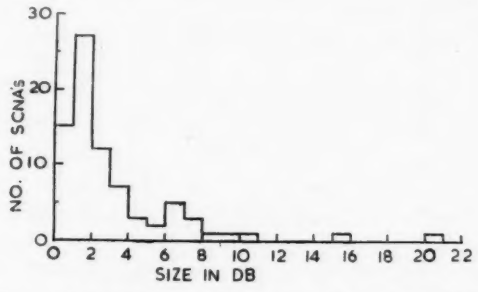

FIG. 3. Frequencies of SCNA's of different intensities.

the distribution lies between 1 and 2 db and that the number of SCNA's falls off rapidly with increasing size. Actually what one might expect is that the number of SCNA's of the smallest size would be the largest. But in practice, this has not been found to be so. It is possible that a few SCNA's of size smaller than 1 db have been missed owing to natural or artificial interference. Besides, it has been observed that all small flares are not capable of causing SCNA's or it may be that, an SCNA once started, always grows to a certain minimum size. A similar type of distribution, in the case of SPA's, was observed by Bracewell and Straker. Shain and Mitra succeeded in showing that the cumulative frequency distribution of SCNA's obeys the following relation,

$$dn = ks^{-p}\, ds \qquad (1)$$

where n is the number of SCNA's in a small range 'ds' of s, where s is the size and k is a constant. They found that a value of p near about 2 gives the

best fit. Figure 4 shows the cumulative frequency distribution of the SCNA's of different sizes observed at Ahmedabad on 25 Mc./s., that is, the percentage

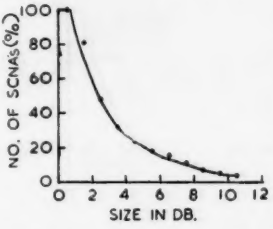

FIG. 4. Cumulative frequencies of SCNA's.

of the total number of SCNA's having a size equal to or greater than a defined amount. Even though the sizes of SCNA's observed at Ahmedabad are larger than those observed in Australia by a factor of about 3, the above relation (1) with p near about 2 still holds.

(*b*) *Time of growth.*—In Table I, the mode, median and quartile values of the times of growth of SCNA's and SPA's are compared. It is evident

TABLE I

Times of growth of SCNA's and SPA's in minutes

Method	Authors	Mode	Median	Quartiles	
				Q_1	Q_3
SCNA 18·3 Mc./s.	Shain and Mitra	..	5	4	9
SPA 16 Kc./s.	Bracewell and Straker	6	7·5	5·5	10·5
SCNA 25 Mc./s.	Bhonsle	5	7	4·7	11·0

that the frequency distribution of the times of growth measured at Ahmedabad agree well with those observed elsewhere. Helen W. Dodson *et al.*[7] attempt to distinguish between sudden short wave fade-outs and gradual short wave fade-outs. According to them, gradual and sudden SID's represent two quite different phenomena. It is possible that the SCNA's of short and long times of growth are associated with sudden and gradual short wave fade-outs respectively.

(*c*) *Duration.*—Table II gives durations of SCNA's and SPA's and summarizes the observations of the other workers. The median and quartile

TABLE II

Durations of SCNA's and SPA's in minutes

Method	Authors	Mode	Median	Quartiles Q_1	Quartiles Q_3
SCNA 18·3 Mc./s.	Shain and Mitra	..	21	15	34
SPA 16 Kc./s.	Bracewell and Straker	30	33	26	48
SCNA 25 Mc./s.	Bhonsle	55	47	27	62

values of duration differ widely at different places. The median value of duration obtained from the observations at Ahmedabad is much larger than those obtained from SCNA's at 18·3 Mc./s. and SPA's at 16 Kc./s. It is interesting that while the times of growth of SCNA's and SPA's are in good agreement, their durations differ. By duration we mean the interval of time between the earliest indication of an SCNA and its end as determined from the appearance of the record. Figure 5 represents a scatter diagram of size

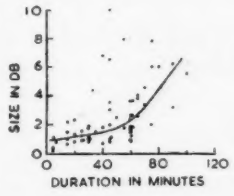

FIG. 5. Scatter-diagram of size and duration of SCNA's.

against duration of SCNA's at Ahmedabad. SCNA's of type C, *i.e.*, multiple or extended ones, are not included in this diagram. There is an obvious tendency for the duration to increase with increasing size of SCNA. In general the SCNA's observed at Ahmedabad take a much longer time to recover than those observed in Australia, and this is probably connected with the difference in the phases of solar activity in which the observations were made.

(*d*) *Ratio* (*Duration/Time of Growth.*)—Waldmeir[8] gave the ratio of the duration of the flare to its time of growth as 5. In Table III a comparison

TABLE III

Ratio (*Duration/Time of growth*) *of SCNA's and SPA's*

Method	Authors	Mode	Median	Quartiles Q_1	Quartiles Q_3
SPA 16 Kc./s.	Bracewell and Straker	4	..	3·5	6·5
SCNA 25 Mc./s.	Bhonsle	4·5	4·7	3·5	7·5

is made between our observations of SCNA's with those of SPA's. There is good agreement in the values of this ratio. This means that, on an average, an SCNA lasts for a period which is about five times the period which it takes to grow to its full size.

6. Changes in Atmospheric Ionization Associated with Solar Flares

Nicolet[10] suggested that the formation of the normal D-region could be explained by the photo-ionization by L_α, and Mitra[9] extended this idea by suggesting that the enhancement of L_α radiation during solar flares was responsible for the increased D-region ionization. He assumed that the flare-time enhancement of ionization occurred uniformly throughout the D-region. In the light of later work on low frequency reflections from the lower ionosphere (Gardner[13]) and rocket observation on solar spectra (Friedman *et al.*[12]), flares do not seem to have any perceptible influence on the E and F layers, but the D-layer is very much affected. Observations of SPA's show that the reflecting ceiling for long waves is lowered by about 15 km. during 3+ flares. The ionization of a substance like NO by L_α seems insufficient to produce such a large lowering of the base of the D-layer. According to Friedman and Chubb, if the lowering of the D region were due to L_α, its intensity in large flares should increase by a factor 10^5. This is highly improbable. The alternative view which is now generally accepted is that, the solar flares emit X-rays and with increase in the size of the flare, increasing amounts of X-rays of the shortest wavelengths ($\lambda\lambda$ 8Å–2Å) are emitted. These rays penetrate the atmosphere down to 70 km. causing ionization of all components of atmospheric air. Gardner and Pawsey's[11] studies of the partial reflections of long waves from the lower ionosphere confirm the

TABLE IV

Solar flare absorptions tabulated from the recordings of cosmic radio noise on 25 Mc./s. at the Physical Research Laboratory, Ahmedabad, India

23rd Feb. 1956 to 14th Sep. 1958

Date	Class of flare according to CRPL	Type of SCNA observed in Ahmedabad	Time of beginning UT	Duration in min.	Time for half-recovery in min.	Maximum absorption in db
1956						
February						
23	3+	B	0331	90	22	6·2
March						
10	2	B	0450	100	25	5·5
May						
30	2+	C, D	0240	180	20	2·1
30	2+	B, C	0940	160	13	8·1
31	3	B, C	0749	50	8	9·2
July						
24	..	B	0920	70	5	4·5
25	..	C	0530	20	4	2·0
25	..	C	0550	20	8	0·8
27	..	A	0540	25	7	1·5
27	..	C	0920	50	7	2·3
August						
27	1	C	0949	15	7	1·5
27	1	C	1002	60	10	1·2
28	1+	A	0805	80	17	6·0
29	2	A, C	0955	150	20	5·3
September						
9	..	A	0745	45	12	6·5

TABLE IV (*Contd.*)

Date	Class of flare according to CRPL	Type of SCNA observed in Ahmedabad	Time of beginning UT	Duration in min.	Time for half-recovery in min.	Maximum absorption in db
November 15	1	B, C	0810	85	8	1·3
18	1	B	0838	55	15	1·8
22	1	A	0855	60	20	1·0
December 17	2	A	1010	30	15	0·8
18	1	A	0405	60	25	1·9
19	..	A, C	0605	95	7	7·6
19	1	A, C	0845	50	17	2·7
20	2	A	0450	55	8	7·9
20	1	A	0635	65	5	3·8
26	2	A	0535	60	5	1·2
27	1	A	0625	30	15	1·9
1957 January 27	..	A	0745	40	10	6·7
February 14	1	B	0422	45	35	1·1
19	..	B, D	0250	5	2	1·1
March 12	..	A	0548	15	5	2·2
April 14	..	A	0536	60	20	1·5
16	3	A	1040	75	30	7·8
20	..	D	0200	15	5	0·7

TABLE IV (*Contd.*)

Date	Class of flare according to CRPL	Type of SCNA observed in Ahmedabad	Time of beginning UT	Duration in min.	Time for half-recovery in min.	Maximum absorption in db
June						
4	..	B	0857	70	25	3·4
10	1	B	1048	60	30	2·6
July						
1	1+	B	0345	40	8	0·7
4	..	B	0435	60	30	0·9
8	2	B	0538	30	8	1·0
12	..	B	0436	25	15	3·9
16	2	B	0737	45	15	3·5
21	2	D	0135	5	2	0·2
21	..	C	0333	5	2	0·4
21	..	C	0416	5	2	0·3
21	..	B	0704	65	30	2·6
22	..	B	0630	45	20	1·0
29	2	C	0456	50	7	1·1
August						
8	2+	B	1122	45	15	1·1
September						
1	1	D	0204	20	10	0·7
3	..	B	1024	45	7	2·0
7	2	B	0815	35	7	15·0
15	1	C	0333	75	30	0·9
18	1	C	0630	60	15	0·8

TABLE IV (*Contd.*)

Date	Class of flare according to CRPL	Type of SCNA observed in Ahmedabad	Time of beginning UT	Duration in min-	Time for half-recovery in min.	Maximum absorption in db
19	2+	B	0803	65	22	4·0
21	1+	C	0415	75	20	1·2
October						
1	1	B	0653	35	8	1·5
19	2	B, C	0632	90	30	1·4
November						
10	2	B	0658	45	15	3·0
17	1+	B	0530	60	15	1·8
23	2	B	0735	60	17	3·6
December						
10	..	A	0435	75	27	2·0
15	..	B	0537	7	3	3·8
17	..	B	0737	90	35	3·2
18	..	B	0625	60	22	1·6
19	2	B	0753	60	17	2·4
20	1	A	0545	?	15	1·1
26	1+	B	0917	45	8	0·8
1958						
March						
11	..	B	0614	15	10	1·0
11	..	B	0717	30	15	1·8
23	3+	B	0955	150	10	20·0
April						
2	2	B	0500	20	5	2·3

TABLE IV (*Contd.*)

Date	Class of flare according to CRPL	Type of SCNA observed in Ahmedabad	Time of beginning UT	Duration in min.	Time for half-recovery in min.	Maximum absorption in db
7	..	B	0652	30	7	1·1
May 5	1+	B	0415	33	7	4·3
June 2	..	B	0700	20	7	1·2
3	..	C	0240	25	7	1·2
6	2	B	0437	40	12	1·8
July 29	3	B	0300	45	17	10·0
August 28	2+	B	1022	75	30	6·0
September 14	2+	B	0853	60	25	2·6

Type A .. Sudden increase in absorption.
B .. Sudden burst of intensity followed by absorption.
C .. Absorption due to multiple or extended flares.
D .. Flare at the time of low sun.
Local Mean Time = UT + $4^h\ 50^m$

existence of two reflecting regions, one near 70 km. and another near 90 km. Gardner[13] showed that even during SID's, this grouping of echo-heights is maintained. He concluded that during an SID, most absorption of E-echo takes place between 85 km. and E-reflection level. The course of an SPA and SCNA during a solar flare need not be the same. SPA's depend mainly on the ionization of the lower D-region but SCNA's are affected by the total absorption which is proportional to $\int N \nu\, dh$, through the ionosphere where N is the number of electrons per unit volume and ν is its collision frequency. Hence, it is to be expected that SCNA's will take more time to disappear than SPA's.

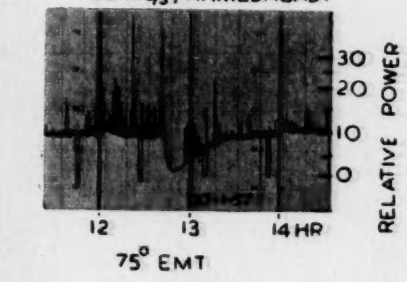
SUDDEN COSMIC NOISE ABSORPTION
25 Mc/s, AHMEDABAD.
30
20
10
0
RELATIVE POWER
12
13
14 HR
75° EMT

FIG. 1 *(a)*

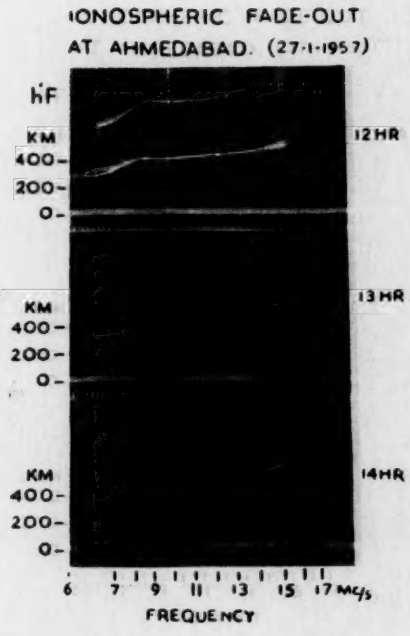
IONOSPHERIC FADE-OUT
AT AHMEDABAD. (27-1-1957)
h'F
KM
400-
200-
0-
12 HR
13 HR
14 HR
6
7
9
11
13
15
17 Mc/s
FREQUENCY

FIG. 1 *(b)*

7. Conclusions

(*a*) SCNA's on 25 Mc./s. observed at Ahmedabad have been classified into four types; Type A, Type B, Type C and Type D. SCNA's of type B are the most common.

(*b*) SCNA's of size between 1 and 2 db are most frequent, and their number falls rapidly with increase in size.

(*c*) The time of growth of SCNA's is generally of the order of 5 min., which is in good agreement with that found by other workers.

(*d*) Durations of SCNA's observed at Ahmedabad is much longer as compared to SPA's. There is an obvious tendency for the duration to increase with increasing size of an SCNA.

Acknowledgements

The author wishes to express his gratitude to Dr. K. R. Ramanathan under whose guidance this investigation has been carried out. He has been in receipt of a Senior Research Fellowship from the Indian Council of Scientific and Industrial Research, Government of India.

References

1. Mitra, A. P. and Shain, C. A. — *J. Atmosph. Terr. Phys.*, 1953, **4**, 204–18.
2. Bhonsle, R. V. and Ramanathan, K. R. — *J. Sci. Industr. Res.*, 1958, **17 A**, 40–45.
3. Shain, C. A. and Mitra, A. P. — *J. Atmosph. Terr. Phys.*, 1954, **5**, 316–28.
4. Bracewell, R. N. and Straker, T. W. — *Mon. Not. R. Astron. Soc.*, 1949, **109**, 28–45.
5. Ramanathan, K. R., *et al.* — *Proc. Ind. Acad. Sci.*, 1956, **43 A**, 306–08.
6. Sarabhai, V., *et al.* .. — *Ibid.*, 1956, **43 A**, 309–18.
7. Dodson, Helen, W., *et al.*.. — *Astrophys. J.*, II Supplement No. 20, 1956, 241–70.
8. Waldmeier, M. .. — *Z. fur Astrophys.*, 1940, **20**, 46.
9. Mitra, A. P. .. — *Scientific Report No.* 60, Ionosphere Research Laboratory, The Pennsylvania State University, 1954.
10. Nicolet, M. .. — *Mem. R. Inst. Met., Belgium*, 1945.
11. Gardner, F. F. and Pawsey, J. L. — *J. Atmosph. Terr. Phys.*, 1953, **3**, 321–44.
12. Friedman, H., *et al.* .. — *IGY Bulletin—Rocket Flare Patrol Programme, Trans. Amer. Geophys. Union*, 1958, **39**, 165.
13. Gardner, F. F. .. — *Aust. J. Phys.*, 1959, **12**, 42–53.

ORE-MICROSCOPIC STUDIES OF THE MANGANESE ORE-MINERALS OF OLD M.P.

II. Satak, Beldongri, Lohdongri and Kachurwahi, Nagpur District

By S. P. Deshpande

(University Department of Geology, Nagpur)

Received June 24, 1959

(Communicated by Prof. Sripadrao Kilpady, F.A.SC.)

Introduction

The paper gives an account of the mineragraphic study of the manganese ore-minerals collected from Satak, Beldongri, Lohdongri and Kachurwahi manganese mines, in Nagpur district (Bombay State). All these four deposits lie approximately on the same line of strike and form a part of the belt of manganese ore-deposits stretching in an easterly direction from Dumri Kalan to Khandala, a total distance of 12 miles, and containing the above-mentioned deposits successively as we go from west to east. The area forms a part of the topographical sheet No. 55 O/7 and lies about four miles to the east of Dumrikhurd railway station which is about 20 miles to the north-east of Nagpur and lies on the Nagpur-Ramtek branch of the S.E. Railway.

J. A. Dunn (1936) was the first to carry out a mineragraphic study of some selected specimens, mainly of Vredenburgite, from L. L. Fermor's (1909) collection of the manganese ores of Beldongri. But apart from this, no systematic mineragraphic study of the ores from the deposits in this belt, has been made hitherto.

Geology of the Area

All the ore-deposits are isolated outcrops in alluvium and are probably hills now submerged in the alluvium of the Sur river.

The ore-deposit at Satak outcrops as a low flat bare mound about $\frac{1}{4}$ mile long and striking E. 10° N. The dip is about 40–50° to the south. There are two parallel ore-bands, both about 7 feet thick and separated by a layer of mica-schist. The wall rocks consist mainly of mica-schists with subordinate gneisses and quartzites.

The Beldongri deposit is situated about a mile E.N.E. of the Satak deposit. The ore-band is about 60 feet thick with an exposure of about 100 yds. The

strike is E. 5° N. at the west-end veering round to E. 40° N. at the east-end. The dip averages about 50–60° to the south. The underlying rocks were not exposed but the overlying rocks consist of schistose micaceous gneisses. Gondites, schists and quartzites are intercalated with the ore-band. Intrusions of felspathic rocks occur in both the Satak and Beldongri deposits (Fermor, 1909). However, at the time of the author's visit, the mine was an abandoned pit with about 70 feet of water. The specimens were collected from the talus ore scattered around the pit.

The deposit at Lohdongri formed a low flat mound about 380 yds. long from east to west, 200 yds. broad and about 30–35 feet thick, which is now largely excavated. The ore layers, striking due east (with a steep dip to the south), vary in thickness from 2 feet to 2 inches and more and are crumpled about axes parallel to the strike. The total thickness of the ore-bands is probably about 60 feet (Fermor, 1909). The underlying (footwall) rocks consist of mica-schists with some quartzites.

The ore-band at Kachurwahi strikes E. 10° N. on an average with a dip of about 60–70° to the south. The ore-band is separated into a number of bands, each about 5–10 feet thick, by layers of quartzites and schists. The hanging wall consists of felspathic mica-schist and the footwall is a mica-quartz-schist. Intrusions of felspar rock are also seen here (Fermor, 1909).

Mineralogy of the Ores

The Satak deposit contains about equal proportions of all the three types of ores found in this area, *i.e.*, the Braunite ore, the Vredenburgite-Braunite ore, and the Sitaparite-Hollandite-Braunite ore. At Beldongri, only the Vredenburgite-Braunite ore is found, while at Lohdongri, only the other two types are found. The Kachurwahi deposit contains both the Vredenburgite-Braunite ore and the Braunite ore.

The mineragraphic study of a number of polished sections, prepared from carefully selected specimens, revealed the presence of the following ore-minerals: Braunite, Sitaparite, Hollandite, Jacobsite, Hausmannite, Manganite, Psilomelane, Pyrolusite and two unidentified minerals. The identifications were based on optical characters under polarised light, reflectivity as measured by the Berek's Slit-microphotometer (in green light in air) and the action of standard etch reagents.

Braunite

The mineral takes a good polish. Colour: Grey with a faint brownish tint. In oil a lilac-brown tint is visible. Reflectivity: Low. The value

for green light being about 18·5–19. Pleochroism : Weak; slightly stronger in oil. Anisotropism: Weak but distinct. Grey to brown colours.

Etch Reactions

Positive.—

H_2O_2 — Slow effervescence. No stain.

H_2O_2 (concentrated) + H_2SO_4 (concentrated)—Faster effervescence. Darkens and produces etch scratches. After 4 minutes develops parting planes.

$SnCl_2$ (saturated) + HCl (concentrated)—Tarnishes permanently light brown and develops etch scratches. Strong action after 4 minutes.

Negative.—HNO_3, HCl, KCN, $FeCl_3$, KOH, $HgCl_2$, Aqua Regia.

Braunite occurs as crystalloblastic aggregates of coarse to fine-grained rounded or elongated grains often with Vredenburgite (this name, wherever it occurs in the paper, refers to the intimate oriented intergrowth of Jacobsite and Hausmannite) occurring as interstitial grains (Fig. 1). It often shows mutual boundary relationship with the Vredenburgite and the Jacobsite and also veins the latter (Fig. 3). Numerous rounded inclusions of Braunite are sometimes seen in Vredenburgite (Fig. 5). In the Sitaparite-Hollandite-Braunite ore, it occurs as distinct bands, often intergrown with Sitaparite and unidentified mineral A in lamellar fashion. It veins Hollandite, mainly along grain boundaries and cleavage planes.

Sitaparite

It takes a good polish. Colour: Light-grey with a distinct yellow tint. The tint changes to brownish in contact with Hollandite. Reflectivity: Low. The value is about 21–22. Pleochroism: Not observed. Anisotropism: Either very weak or isotropic. Some grains show beautiful polysynthetic twinning in one or more directions, often forming a complicated mesh.

Etch Reactions

Positive.—

$SnCl_2$ (saturated) + HCl (concentrated)—Etches strongly with the development of etch scratches and a light-brownish stain.

H_2O_2 (concentrated) + H_2SO_4 (concentrated)—Produces weak etch scratches.

HF (concentrated)—Develops texture. Produces slight etch scratches and stains faintly light-brown.

Negative.—HNO_3, HCl, HNO_3 (concentrated), HCl (concentrated), KCN, $FeCl_3$, KOH, $HgCl_2$, H_2O_2, Aqua Regia.

Sitaparite [though the mineral Sitaparite has been shown to be identical with Bixbyite by Mason (1942), he thinks it desirable to retain the name Sitaparite for the specimens occurring in the metamorphosed manganese ores (Mason, 1944). The name Sitaparite is, therefore, retained in this paper] often shows an idioblastic habit. It occurs as bands containing coarse to medium-grained crystalline aggregates of subhedral crystals, in the Hollandite-Sitaparite-Braunite ore. It is often intergrown with Braunite and the unidentified minereal A in lamellar fashion. It also shows euhedral crystal outlines against the Hollandite and the Braunite.

One peculiar occurrence of Sitaparite has been observed in an ore from Beldongri. It shows a light-grey colour with a distinct pinkish yellow tint in oil and very weak anisotropism with dirty pink, yellowish, greenish and grey colours. It occurs as medium to fine-grained crystalline aggregates of irregular grains included in very coarse-grained crystals of Hausmannite (Fig. 6). Jacobsite (with a few Hausmannite lamellæ) also occurs as similar inclusions in Hausmannite. Very small grains of Jacobsite are sometimes included in this Sitaparite. The association of Sitaparite with Vredenburgite is very peculiar (as they belong to different suites) and the author has not seen it reported anywhere. However, the mineral under consideration may not be Sitaparite because it shows a slightly different colour and gives an entirely different reaction with $SnCl_2$ (saturated) + HCl (concentrated). While the reagent produces distinct etch scratches on Sitaparite, it attacks this mineral very strongly, scratches it heavily and turns it nearly completely black. The reaction of H_2O_2 (concentrated) + H_2SO_4 (concentrated) on this mineral is also distinctly stronger than on ordinary Sitaparite.

It is possible that in this particular association the composition of the Sitaparite might be different and hence shows variation in properties. But it is noticed that even a wide range in the composition of Sitaparite has got very little effect on its properties (Mason, 1942). So it is possible that the mineral is not Sitaparite but might be the original alpha-Vredenburgite, in which the dissociation in the two component phases (*i.e.*, Jacobsite and Hausmannite) did not take place. Van Hook and Keith (1958) state that the tetragonal mineral reported by Mason (1943 *b*) as alpha-Vredenburgite might be cation deficient and hence occurs as a single phase instead of as an intergrowth and the existence of single phase metastable mineral in the composition range of Vredenburgite is possible but we would expect it to be cubic if the cation : oxygen ratio is stoichiometric. This view can explain the

isotropic or very weakly anisotropic character of the mineral under consideration. X-ray diffraction studies only, which are to be carried out shortly, can perhaps throw light on the real nature of this mineral.

Hollandite

Sections showing a well-developed prismatic cleavage take a fairly good polish. Other sections are very difficult to polish. Colour: Grey-white to white. A faint yellowish tint is visible in oil. Reflectivity: Moderately high. The value varies from 28–30. Pleochroism: Distinct in oil. Anisotropism: High. Yellowish, purplish, greenish and bluish-grey colours. Badly polished sections with no cleavage show weak anisotropism and pale violet pink, dark violet grey, greyish brown and bluish grey colours. Cleavage in one direction is well developed in some grains.

Etch Reactions

Positive.—

$SnCl_2$ (saturated) + HCl (concentrated)—Etches heavily. Brings out close lamellar striations and cleavage. Effect very strong on sections with no cleavage. These sections get almost completely black. Drop of the reagent turns yellow.

H_2O_2 (concentrated) + H_2SO_4 (concentrated)—Vigorous effervescence. Blackens and brings out cleavage and grain boundaries. Effect very strong on sections with no cleavage.

H_2O_2 (dilute)—Slow effervescence. Slightly attacks sections with no cleavage.

Negative.—HNO_3, HCl, HNO_3 (concentrated), HCl (concentrated), Aqua Regia, KCN, $FeCl_3$, KOH, $HgCl_2$.

Hollandite occurs as a crystalline aggregate of medium to coarse-grained and stout prismatic subhedral crystals usually occurring as well-defined bands alternating with those of Braunite, Sitaparite and occasionally the unidentified mineral A (Fig. 8). Pyrolusite and Psilomelane often vein and replace Hollandite along the grain boundaries and the cleavage planes. Braunite also veins Hollandite mianly along the grain boundaries and the cleavage planes.

Unidentified Mineral A

It takes a good polish. Colour: Grey with a faint yellowish tint. Reflectivity: Low. The value is about 19·5–20·5. Pleochroism: Not observed. Anisotropism: Very weak. Greenish yellow-brown to grey colours. No internal reflections observed.

Etch Reactions

Positive.—

$SnCl_2$ (saturated) + HCl (concentrated)—Produces etch scratches and stains permanently light-brown.

H_2O_2 (concentrated) + H_2SO_4 (concentrated)—Produces weak etch scratches and a light-brownish stain.

HF (concentrated)—Produces weak etch scratches.

Negative.—HNO_3, HCl, HNO_3 (concentrated), HCl (concentrated), Aqua Regia, H_2SO_4 (concentrated).

The mineral occurs as a crystalline aggregate of medium to coarse-grained grains. It forms distinct bands alternating with those of Braunite, Sitaparite and Hollandite, and its grains are always coarser than those of the associated Braunite and Sitaparite. It is often intergrown with Braunite and Sitaparite in lameller fashion. In the bands of this mineral, lamellar or irregular but oriented inclusions of some gangue mineral are found (Fig. 8). The gangue mineral is either forming a lamellar intergrowth with this mineral (because wherever Braunite is also intergrown with the same crystals its lamellæ are parallel to those of the gangue mineral) or the unidentified mineral A has been formed by the oriented replacement of this gangue mineral and the lamellar inclusions of the gangue mineral are the leftovers after replacement. Which of these two interpretations is correct is difficult to determine.

A similar mineral was found in the ores of Gowari Warhona and was fully described in a previous paper (Deshpande, 1959).

The unidentified mineral A has got properties (like the mineral from Gowari Warhona) intermediate between those of Braunite and Sitaparite but it differs from the latter in showing weaker pleochroism and giving slightly different etch reactions; but they mainly differ in one important respect. In the ores of Gowari Warhona a very fine intergrowth of Braunite and Sitaparite was observed, which had properties intermediate between those of Braunite and Sitaparite, and it was suggested that the mineral might have originated from the intergrowth (though for other reasons it was thought that the mineral was quite distinct from such an intergrowth), but in these ores from Satak no fine intergrowth of Braunite and Sitaparite, which could have led to the formation of the unidentified mineral A, was noticed. The oberved intergowth between Braunite and Sitaparite was quite coarse and distinct and was comparatively rare. The mineral from Gowari Warhona was thought to be probably Alpha-Vredenburgite but this unidentified

mineral cannot be Alpha-Vredenburgite because it shows a very weak anisotropism and might be regarded as isotropic at times. It may be a variety of Sitaparite or possibly a different mineral having affinities with Sitaparite and Braunite. The real nature of this mineral can only be unravelled by X-ray diffraction analysis.

Jacobsite

It takes a fairly good polish. Colour: Grey with a distinct yellowish olive tint. In contact with Hematite, the tint is brownish yellow. In some specimens from Beldongri, a pinkish yellow tint is seen in addition and there is often an irregular transition from this to the yellowish olive tint. Reflectivity: Low, the value being about 19·5–20. Pleochroism: Not observed. Anisotropism: Very weak or isotropic. Red internal reflections are occasionally visible in oil.

Etch Reactions

Positive.—

$SnCl_2$ (saturated) + HCl (concentrated)—Occasionally darkens slightly and produces very weak etch scratches but mostly negative.

HF (concentrated)—Develops texture (Fig. 5). Produces etch scratches, blackens differentially and stains light olive.

Negative.—Negative to all other standard etch reagents.

Jacobsite occurs in these ores in two ways. Firstly it occurs as rounded medium to coarse-grained crystalline aggregates (containing Hausmannite lamellæ) interstitial to those of coarse-grained Braunite (Fig. 1). Such Vredenburgite also often shows mutual boundary relationship with the Braunite and contain numerous small rounded inclusions of Braunite (Fig. 5). Secondly, it occurs as rounded medium to coarse-grained crystalline aggregates (Hausmannite-free) showing mutual boundary relationship with the Braunite. Secondary Braunite and Hematite also clearly vein Jacobsite in this ore (Fig. 3).

Hausmannite

The mineral takes a good polish. Colour: Light-grey to dark-brownish grey. Reflectivity: Low. The value is about 20–21. Pleochroism: Distinct. Anisotropism: Strong. Yellowish grey, bluish grey and brownish grey colours. Numerous scratches are visible in the lightest position. Coarse lamellar twinning in one or more directions is observed. The lamellæ are often intersecting and are of unequal width. At places small lamellæ are arranged diagonally between two adjacent principal lamellæ

and the structure resembles that of a distorted ladder (Fig. 6). Red internal reflections are abundant in oil.

Etch Reactions

Positive.—

HCl (concentrated)—Etches weakly. Develops texture.

$SnCl_2$ (saturated) + HCl (concentrated)—Darkens and develops twinning planes.

H_2O_2 (concentrated) + H_2SO_4 (concentrated) — Same as above. Also produces slight etch scratches.

H_2O_2—Effervescence. Surface unaffected.

Negative.—HNO_3, HCl, HNO_3 (concentrated), H_2SO_4 (concentrated), Aqua Regia, KCN, $FeCl_3$, KOH, $HgCl_2$.

Hausmannite usually occurs as lamellæ in the octahedral directions of Jacobsite grains (Figs. 1, 2, 5). It also occurs as irregular seggregations of medium to coarse-grained crystals in the Jacobsite. Occasionally, it forms extremely coarse-grained granoblastic aggregates of rounded subhedral crystals. Medium to fine-grained and irregular inclusions of Vredenburgite and Sitaparite (?) are found in them (Fig. 6). Hausmannite is always largely replaced and veined by Psilomelane often along the twinning planes.

Manganite

It takes a good polish. Colour: Light-grey to dark-brownish grey with olive tint in one position. Reflectivity: Low. The maximum and minimum reflectivity values are 19·5 and 16 respectively. Pleochroism: Very strong. Anisotropism: Very strong. Yellowish, bluish grey and dark-violet grey colours. Internal reflections are red and are quite abundant in oil. One directional prismatic cleavage is visible in some coarser needles.

Etch Reactions

Positive.—

HCl (concentrated)—Produces slight etch scratches.

$SnCl_2$ (saturated) + HCl (concentrated)—Etches heavily. Blackens considerably.

H_2O_2 (concentrated) + H_2SO_4 (concentrated)—Tarnishes strongly. Brings out grain boundaries and probably cleavage in some grains.

Negative.—HNO_3, HCl, HNO_3 (concentrated), Aqua Regia, H_2SO_4 (concentrated), KCN, $FeCl_3$, KOH, $HgCl_2$.

Manganite forms finely crystalline aggregates of thin prismatic needles which are sometimes radiating. It veins Braunite, Jacobsite, Hausmannite and the gangue minerals often along with Pyrolusite and Psilomelane. It also replaces the gangue minerals. Pyrolusite often replaces it mainly along the cleavage planes and also forms pseudomorphs after it.

Psilomelane

It takes a good polish. Colour: Greyish white to bluish grey. A brownish tint is seen in some specimens. Reflectivity: Moderate. The value is about 26–28. Pleochroism: Distinct. Anisotropism: Strong. Yellowish white to grey colours. Undulose extinction often visible.

Etch Reactions

Positive.—

HNO_3—Stains light-brown. Some specimens negative.

HCl—Stains permanently brown.

H_2O_2—Strong effervescence. No stain.

$SnCl_2$ (saturated) + HCl (concentrated)—Etches completely black.

H_2O_2 (concentrated) + H_2SO_4 (concentrated)—Etches completely black.

Negative.—Aqua Regia, KCN, KOH, $HgCl_2$.

Psilomelane usually occurs as extremely fine-grained and almost cryptocrystalline aggregates but occasionally it forms fine-grained needles (sometimes fibrous) showing strong anisotropism. It replaces some of the gangue minerals metasomatically and in these replacements it shows coarse-grained form with strong anisotropism. It veins and replaces Hausmannite (often along the twinning planes), Braunite (mostly along the grain boundaries), Hollandite (mostly along the grain boundaries and the cleavage planes), Jacobsite and the gangue minerals. It often gives rise to Pyrolusite after dehydration.

In the vugs of an ore from Beldongri, Psilomelane is found showing a brownish grey colour, high anisotropism and stout prismatic habit with probably a one-directional cleavage at places. It is associated with Pyrolusite which shows a similar habit. The author believes that the Psilomelane has replaced the Pyrolusite (mainly along the cleavage planes) and has formed pseudomorphs after it.

Unidentified Mineral B

It takes a good polish. Colour: Yellowish white to grey. Colour slightly uneven at places. Reflectivity: Moderate. Maximum reflectivity

slightly lower than that of Pyrolusite and minimum reflectivity slightly higher than that of Psilomelane. The value varies from 28–30. Pleochroism: Distinct. Anisotropism: Strong. Pinkish white and brownish yellow to dark brownish-grey colours.

Etch Reactions

Positive.—

HCl—Darkens slightly or negative.

$SnCl_2$ (saturated) + HCl (concentrated)—Etches completely black. Reaction slower than for Psilomelane.

H_2O_2 (concentrated) + H_2SO_4 (concentrated)—Etches completely black. Reaction faster than for Pyrolusite.

Negative.—HNO_3, HNO_3 (concentrated), HCl (concentrated), H_2SO_4 (concentrated), Aqua regia, KCN, KOH, $HgCl_2$.

The mineral occurs as coarse-grained irregular grains associated with Pyrolusite and Psilomelane in the vugs of an ore from Beldongri already referred to in the description of Psilomelane. It is excessively veined by Psilomelane. The grains at places show colloform outlines (Fig. 7).

The mineral shows properties which are intermediate between those of Pyrolusite and Psilomelane. But its coarse-grained nature and strong anisotropism (with typical anisotropic colours) clearly distinguishes it from both Psilomelane and Pyrolusite. X-ray diffraction analysis of this mineral is expected to throw light on the identity of this mineral.

Pyrolusite

The mineral polishes with difficulty. Colour: White with a yellow tint to grey-white. Reflectivity: Moderately high. The value varies from 34–39. Pleochroism: Distinct. Anisotropism: Strong. Yellowish, yellow-brown, greenish blue and grey colours. Four distinct extinctions per revolution are seen. Some needles show undulose extinction. A well-marked one-directional prismatic cleavage often seen.

Etch Reactions

Positive.—

H_2O_2—Strong effervescence. No stain.

$SnCl_2$ (saturated) + HCl (concentrated)—Etches instantaneously black.

H_2O_2 (concentrated) + H_2SO_4 (concentrated)—Etches completely black. Reaction slower than for Psilomelane.

H_2SO_4 (concentrated)—Tarnishes some specimens permanently brown.

Negative.—HNO_3, HCl, HCl (concentrated), HNO_3 (concentrated), Aqua Regia, KCN, KOH, $HgCl_2$.

Pyrolusite usually occurs as medium to fine-grained aggregates of stumpy prisms veining the earlier-formed manganese minerals. It also replaces Psilomelane and Manganite, the latter often along the cleavage planes. Crystalline aggregates of medium-grained Pyrolusite (often altered to Psilomelane) occur interstitially to Braunite in the Braunite-Vredenburgite ore and Braunite forms a raction rim between Pyrolusite and Vredenburgite in these ores (Fig. 2).

TEXTURAL FEATURES

The manganese ores of this area occur in the following mineralogical assemblages:—

(*a*) Braunite Ore.

(*b*) Sitaparite-Hollandite-Braunite Ore.

(*c*) Jacobsite-Hausmannite-Braunite Ore.

The textural relationships of the minerals in these assemblages will now be considered.

(*a*) *Braunite Ore.*—In this ore Braunite forms coarse to fine-grained aggregates of rounded anhedral crystals. The ore is often traversed by innumerable veinlets of Psilomelane which are veining and replacing the Braunite mostly along the grain boundaries of the latter. Replacement of Psilomelane has given rise to Pyrolusite at many places. The ore sometimes shows a rough banded texture with coarse-grained Hematite occurring interstitially to Braunite in certain bands. Fine veinlets of Hematite are given off from these bands into the Braunite.

In the vugs and open spaces in this ore, coarse-grained Pyrolusite, unidentified mineral B and Psilomelane have been deposited, at places. It appears that the first two have been deposited earlier, and later Psilomelane veins and replaces them. Psilomelane is probably pseudomorphous after Pyrolusite at places.

(*b*) *Sitaparite-Hollandite-Braunite Ore.*—The typical ore of this type shows a crystalloblastic banded texture of a metamorphic rock. Bands of Hollandite, Braunite, Sitaparite and occasionally those of the unidentified mineral A, alternate. Hollandite forms medium to coarse-grained subhedral prismatic grains which are roughly parallel to the banding. Braunite, forming medium to fine grained-aggregates of rounded anhedral cystals,

shows concave outlines towards Hollandite. Sitaparite forms medium to fine-grained aggregates of euhedral to subhedral crystals and shows crystal outlines against both Braunite and Hollandite. Braunite and Sitaparite are often intergrown in a lamellar fashion. Wherever the unidentified mineral A is found in these ores, it forms coarse-grained aggregates of anhedral to subhedral grains with abundant lamellar or irregular inclusions of some gangue mineral. Braunite and Sitaparite also form lamellar intergrowths with the unidentified mineral A. Where Braunite is intergrown with grains of the unidentified mineral A containing lamellar inclusions of gangue, the lamellæ of Braunite and those of the gangue mineral are parallel. Minute Hollandite inclusions are abundant in both Braunite and Sitaparite but are rarely found in the unidentified mineral A.

Psilomelane veins and replaces Braunite and Hollandite mainly along the grain boundaries and the latter also along the cleavage planes. Braunite also veins Hollandite mainly along the grain boundaries and the cleavage planes.

(*c*) *Jacobsite-Hausmannite-Braunite Ore.*—In the typical ore, Braunite forms medium to very coarse-grained granoblastic aggregates of rounded anhedral grains. Medium to coarse-grained Vredenburgite is crystallised in the interstices of the earlier formed Braunite grains. At places the Vredenburgite extends out as long narrow zones between the Braunite grains. In the Vredenburgite, the Hausmannite lamellæ occupy the octahedral directions in the crystals of Jacobsite which occur as groundmass. Irregular medium to coarse-grained crystals of Hausmannite are also included in the Jacobsite. Occasionally, Hausmannite forms extremely coarse-grained aggregate of rounded subhedral grains with medium-grained inclusions of Vredenburgite and probably Sitaparite. This Sitaparite (?) in turn sometimes contains minute inclusions of Jacobsite.

Vredenburgite also sometimes shows mutual boundary relationship with Braunite and this Vredenburgite is often quite coarse-grained and contains innumerable minute and rounded inclusions of Braunite. Later Braunite also veins the Jacobsite.

Occasionally we get Hausmannite-free Jacobsite showing mutual boundary relationship with the Braunite. Hematite veins both the Jacobsite and the Braunite and sometimes forms coarse-grained irregular grains showing twinning. Braunite veins Jacobsite in this ore.

Braunite often forms a sort of a reaction rim between Jacobsite and some gangue mineral and also between Jacobsite and Pyrolusite. Aggregates of Pyrolusite crystals are found only in the Braunite areas and they are never

found in contact with Jacobsite. This Pyrolusite is often altered to Psilomelane. Dunn (1936) had recorded the reaction rim of Braunite formed between the Jacobsite and the Pyrolusite in his studies of the Beldongri ores, but the reaction rim of Braunite between the Jacobsite and the gangue mineral (found in the ores from Satak) has hitherto not been reported. It will be discussed more fully while discussing the paragenesis and origin of the ores.

Psilomelane, Pyrolusite, Manganite and occasionally Hematite vein Jacobsite, Braunite, Hausmannite and the gangue. Psilomelane also replaces Hausmannite mainly along the twinning planes and also the gangue along with Manganite.

PARAGENESIS

The textural characteristics of the ores described above provide sufficient evidence towards the interpretation of the order of formation of the various minerals and also to some extent of their origin.

Starting with the Vredenburgite-Braunite ore, it can be inferred that the Braunite was the first mineral to crystallise in the earlier phases of the regional metamorphism when the temperature and the pressure was increasing. The Pyrolusite, crystallised in the interspaces of the Braunite grains, was probably introduced by hot solutions in these earlier phases. The impurities in the ore formed some gangue minerals along with Braunite. As the intensity of the metamorphism increased, Jacobsite containing Mn_3O_4 in solid solution started crystallising in the interspaces of the Braunite. Wherever Jacobsite crystallised along with Pyrolusite and one of the gangue minerals which was chemically unstable at the contact, Braunite was formed as a reaction rim probably in the declining phases of the metamorphism. As the conditions of the metamorphism gradually declined, Hausmannite was exsolved from the Jacobsite which originally contained excess of Mn_3O_4 in solid solution, and it occupied the octahedral directions in the Jacobsite. According to Dunn (1936), this ore might have suffered later metamorphism whereby Hausmannite was seggregated into larger grains leaving wide areas of Jacobsite clear.

Where Mn_3O_4 was far in excess of Fe_3O_4, we encounter large crystals of Hausmannite, obviously formed in the slow cooling process, containing inclusions of previously formed Vredenburgite and Sitaparite (?).

The Sitaparite-Hollandite-Braunite-unidentified mineral A assemblage was probably stable in the medium grade of the regional metamorphism. Sitaparite, showing euhedral crystal outlines against both Hollandite and Braunite obviously started crystallising first. Hollandite, showing euhedral

outlines against Braunite started crystallising a little later, and Braunite, conforming to the outlines of Hollandite crystals, was the last to form. The Sitaparite-Braunite lamellar intergrowth suggests that they were formed contemporaneously and hence we can say that though most of the Braunite was later than Hollandite, it enjoyed a longer period of crystallisation which overlapped that of Sitaparite. The unidentified mineral A, showing lamellar intergrowth with both Braunite and Sitaparite, was probably contemporaneous with the Braunite-Sitaparite intergrowth, but the possibility that it was formed by the oriented replacement of the earlier formed gangue cannot be excluded. Later Braunite veined (and to some extent replaced) all the earlier formed minerals in the declining phases of the metamorphism.

Exactly what conditions led to the formation of the Sitaparite-Hollandite-Braunite ore on one hand and the Jacobsite-Hausmannite-Braunite ore on the other hand cannot be inferred with any certainty. It is definitely not correct to say that the former prevailed in the medium grade (or even in the oxidising conditions) and the latter in the high grade (or in the reducing conditions) of regional metamorphism, as no transition from one to the other is found, and therefore, apparently they are distinct suites of ores. This lack of transition might be due to the shortcomings in the way the ore-specimens were collected and we may perhaps be able to get specimens containing both types of ores which will facilitate a better understanding of their exact relationship. In the absence of such data, we can only say that in the formation of the Sitaparite-Hollandite-Braunite ore, lateral pressure played a very significant part and there was complete obliteration of previously formed minerals with consequent rearrangement in which Sitaparite started crystallising first, Hollandite a little later and Braunite still later, though for a considerable part their periods of formation overlapped. On the other hand, the Jacobsite-Hausmannite-Braunite ore was formed under deep-seated conditions where uniform pressure takes the place of directed pressure. Earlier formed minerals like Braunite recrystallised to form coarse-grained aggregates and Vredenburgite was crystallised in the interspaces of the Braunite grains, the periods of formation of both the minerals overlapping slightly. With uniform pressure prevailing, all the traces of banding, etc., disappeared and the ore assumed a granular texture. Dunn (1936) had reported Vredenburgite-Braunite with a similar texture which he says can also form from igneous melts and that such a possibility cannot be ignored. But the author believes that the assumption of a granulitic stage of metamorphism (highest grade) can very well explain the formation of the texture, and therefore it may be quite unnecessary to introduce the idea of igneous origin for ores which have been repeatedly proved to be undoubtedly of metamorphic origin

Psilomelane, Pyrolusite, Manganite and Hematite vein all the previously formed minerals and are obviously of later formation. Manganite is replaced by later Pyrolusite.

The unidentified mineral B, deposited in vugs and open spaces of the earlier formed minerals, is probably contemporaneous with the other secondary minerals. Later Psilomelane veins it. Psilomelane often gives rise to Pyrolusite after dehydration.

The paragenesis based on textural features and the conditions of formation is given below:—

Conditions of formation	Ore-minerals	Time—→ Primary	Secondary
Medium-grade Metamorphism (Directed pressure prevailing)	Braunite	——— —	..
	Pryolusite	—	———
	Sitaparite	——	..
	Unidentified mineral A	——	..
	Hollandite	——	..
High-grade Metamorphism (Uniform pressre prevailing)	Braunite	——— —	..
	Jacobsite	——	..
	Hausmannite	——	.
Secondary minerals after the decline of Metamorphism	Manganite	..	———
	Unidentified mineral B	..	———
	Psilomelane	..	———
	Pyrolusite	..	———

SUMMARY

The paper gives an account of the mineragraphic study of the manganese ore-minerals collected from Satak, Beldongri, Lohdongri and Kachurwahi manganese mines in Nagpur District, Bombay State. The ore-minerals identified in polished sections are Braunite, Sitaparite, Hollandite, Jacobsite,

Hausmannite, Manganite, Pyrolusite and Psilomelane. In addition, two unidentified minerals have been fully described and the problem of their nomenclature is discussed. Unusual textural features such as the reaction rim of Braunite between Jacobsite and Pyrolusite and Jacobsite and gangue have been described along with a detailed description of the more common textural features. The mineral paragenesis, based on textural features and physico-chemical considerations, has been determined. It is followed by a short discussion on the relationship of the ore-mineral assemblages and the type of metamorphism they have suffered.

Acknowledgements

The author is greatly indebted to Prof. Sripadrao Kilpady, Head of the Department of Geology, Nagpur University, for his kind guidance and valuable suggestions. The author is also indebted to the Government of India for the award of a Senior Research Training Scholarship and the C.P.M.O. Co., for kindly permitting the author to visit their mines and collect specimens.

References

Deshpande, S. P. .. "Ore-microscopic study of the manganese ore-minerals of Gowari Warhona, Chhindwara District, M.P.," 1959, (To be published shortly).

Dunn, J. A. .. "A study of some microscopical aspects of Indian manganese ores," *Trans. Nat. Inst. Sci. Ind.*, 1936, **1** (7), 106–24.

Fermor, L. L. .. "The manganese ore deposits of India," *Memoir, G.S.I.*, 1909, **37** (4), 899–929.

Mason, B. .. "Bixbyite from Langban, the identity of bixbyite and Sitaparite," *Geol. Foren. Forhandl.*, 1942, **64**, 117–25.

———— .. "Mineralogical aspects of the system FeO-Fe_2O_3-MnO_2-Mn_2O_3," *Ibid.*, 1943 *a*, **65**, 97–180.

———— .. "Alpha-Vredenburgite," *Ibid.*, 1943 *b*, **65**, 263–70.

———— .. "The system Fe_2O_3-Mn_2O_3; some comments on the names Bixbyite, Sitaparite, Patridgeite," *Am. Mineralogist*, 1944, **29**, 66–69.

Van Hook, H. J. and Keith, M.L. "The system Fe_3O_4-Mn_3O_4," *Ibid.*, 1958, **43**, 69–83.

Explanation of Plate IV

Fig. 1. Vredenburgite (V) occurring interstitially between the Braunite (B) grains. Etched with $SnCl_2$ (saturated) + HCl (concentrated). Oil immersion, × 90.

Fig. 2. Braunite (B) occurring as a reaction rim between Pyrolusite (black) and Vredenburgite (V). Etched with $SnCl_2$ (saturated) + HCl (concentrated). Oil immersion, × 90.

FIG. 3. Braunite (B) veining Jacobsite (J). Etched with HF (concentrated). Oil immersion, × 210.

FIG. 4. Braunite (B) occurring as a reaction rim between Jacobsite (J) and gangue (black). Etched with HF (concentrated). Oil immersion, × 210.

FIG. 5. Minute rounded inclusions of Braunite (B, white) in coarse-grained Vredenburgite (V, grey). Braunite (B_1) also occurs as a reaction rim between Vredenburgite and gangue (black). Oil immersion, × 90.

FIG. 6. Inclusion of Sitaparite (big dark grain near the centre) in Hausmannite (H). Hausmanite shows complicated polysynthetic twinning. Crossed nicols. Oil immersion, × 210.

FIG. 7. Strongly anisotropic grains of the unidentified mineral B (white) being replaced and veined by Psilomelane (black). Crossed nicols. Oil immersion, × 155.

FIG. 8. Oriented and at places irregular inclusions of gangue (black) in the Unidentified mineral A (grey). A few inclusions of Hollandite (white) are also seen. Oil immersion, × 90.

FIG. 1

FIG. 2

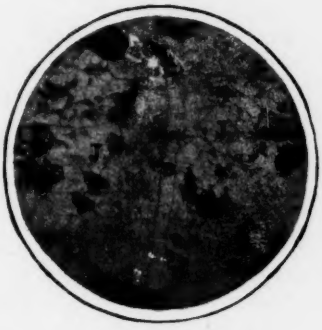

FIG. 3

FIG. 4

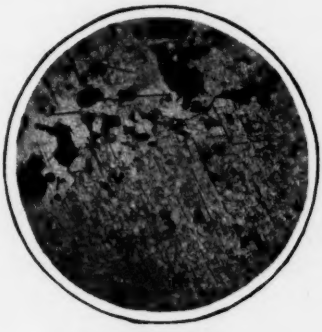

FIG. 5

FIG. 6

FIG. 7

FIG. 8

FIGS. 1–8

ELECTRONIC TRANSITION MOMENT VARIATION IN ($B^1\Sigma \rightarrow X^1\Sigma$) BANDS OF BeO

By N. R. Tawde, F.A.Sc. and N. Sreedhara Murthy*

(Department of Physics, Karnatak University, Dharwar)

Received May 25, 1959

1. Introduction

The object of the present investigation is to undertake an experimental study on vibrational intensity distribution in electronic bands, and put the data to rigorous test in the light of the recent theoretical developments, particularly with reference to the behaviour of the electronic transition moment variation with internuclear separation r. The band system chosen for study is the BeO ($B^1\Sigma \rightarrow X^1\Sigma$) system, particularly because of its astrophysical interest. The related oxides too of alkaline earths are of similar interest in stellar sources (Davis, 1947). Much work so far done on this system (Johnson and Dunstan, 1933, Tawde and Hussain, 1949) pertains only to estimation of peak intensity values of the band heads. This is not of much consequence for such finer theoretical aspects as the rôle of electronic transition moment R_e in vibrational transition probabiltiies. Shuler (1950, 1952) has noted that knowledge of variation of R_e with r is a very important factor in any theory of vibrational transition probabilities. This relation is not yet available in the case of BeO ($B \rightarrow X$) system. It is therefore proposed to investigate it here and this involves both experimental and theoretical intensities. Experimental study is proposed to be done by accurate quantitative measures of intensities under intensity contours of unresolved bands. This technique and the relevant theoretical aspects of electronic transition moments are briefly described in the following sections.

2. Experimental

The BeO ($B \rightarrow X$) band system has been excited in a steady carbon arc at atmospheric pressure with pure beryllium (E. Merck, Dermstadt) packed in lower positive carbon electrode. The electrical parameters of the arc are maintained constant throughout the observations. The band system has been photographed on a Hilger glass prism spectrograph with a dispersion

* Now on the staff of the Department of Physics, Central College, University of Mysore, Bangalore.

ranging from 23·3 Å/mm. at λ 4425 Å to 57·4 Å/mm. at λ 5485 Å. The technique of photographic photometry is followed for the quantitative estimation of integrated intensities (Elliott, 1933; Elliott and Cameron, 1934; Tawde and Patankar, 1943). A stepslit and a standard lamp with known energy distribution have been employed for impressing the calibration marks. The spectra are micro-photometered as usual and overlapping, if any, eliminated by careful extrapolation. Each trace of blackening contour of a band has been converted to intensity contour point by point over the whole band and a new intensity wavelength curve prepared with the help of characteristic curves. The area under the contour is computed by means of a planimeter and the necessary corrections applied. The intensities of the bands are ultimately expressed in terms of the energy units of the standard lamp and put on a relative scale with (0, 0) band as 100 units. A large number of plates have been taken to test the reproducibility of results.

The observed intensities I have been used to compute the I/ν^4 values which are taken as the experimental transition probabilities. These have been compared with theory. The theoretical methods of deriving the transition probability are indicated briefly in the following sections.

3. THEORETICAL

Methods Involving Constancy of Electronic Transition Moment

The intensity, I_{em} in emission is given by

$$I_{em}^{v',v''} = A\nu^4 N_{v'} \bar{R}_e^2 \left[\int \psi_{v'}(r)\ \psi_{v''}(r)\ dr\right]^2.$$

Here, $\int \psi_{v'}(r)\ \psi_{v''}(r)\ dr$ is called the overlap integral and its square gives the transition probability or Franck-Condon factor. $\bar{R}_e$ is assumed to vary slowly with r and thus $\bar{R}_e$ is written as the average value of it.

(*a*) *Analytical methods using simple harmonic wave function*

(*i*) *Hutchisson's method.*—The overlap integral for symmetric molecules, of Hutchisson (1930) with applicability extended by Dunham (1930) to asymmetric molecules involves among others the constant C_3, which has been recently corrected by Tawde, Patil and Savadatti (1959). It has been used here for computations of transition probabilities.

(*ii*) *Manneback's method.*—The calculations by the above method of Hutchisson have been confirmed from the recurrence relations provided by Manneback (1951). The equivalence between the two treatments has been recently shown by Tawde, Patil, Sreedhara Murthy and Katti (1957). The

results by the two treatments are expected to be identical according to them. Although both the Hutchisson's and Manneback's methods are analytical, the latter offers a less laborious, simpler and hence a quicker process of theoretical calculations.

(*b*) *Methods using anharmonic wave functions*

(*i*) *Distortion of harmonic to Morse wave functions.*—In this method, the harmonic wave functions are distorted so as to approximate to anharmonic conditions in the manner shown first by Gaydon and Pearse (1939) and later modified and refined by Pillow (1951). This latter has been followed here for the evaluation of the overlap integral graphically.

(*ii*) *Direct use of Morse potential in the wave functions.*—The details of the treatment and its application to the calculation of overlap integrals of the bands of this system are given in an independent paper by Tawde and Sreedhara Murthy (1959). These calculations have been extended to a few more bands in the meantime and have been used for the purposes of the present problem.

The molecular constants needed for the theoretical calculations of vibrational transition probabilities are taken from the compilation of Herzberg (1950).

4. Results and Discussions

(*i*) *Experimental results*

The final corrected values of relative integrated intensities I of bands of BeO ($B \rightarrow X$) system have been entered in column 2 of Table I. Utilizing

TABLE I

BeO ($B \rightarrow X$) system

Band v', v''	Integrated intensity I	I/ν^4	Band v', v''	Integrated intensity I	I/ν^4
0, 0	100	49·21	2, 1	3·66	1·44
0, 1	17·7	11·57	2, 2	33·2	17·01
0, 2	0·51	0·45	2, 3	17·3	11·66
1, 0	3·95	1·52	2, 4	0·71	0·64
1, 1	62·8	31·51	3, 2	2·76	1·11
1, 2	23·9	15·89	3, 3	16·6	8·64
1, 3	0·84	0·75	3, 4	12·3	8·38
			3, 5	0·97	0·88

the wavelength measurements of Lagerqvist (1948), I/ν^4 values have been obtained in each case. These have been entered in column 3 of the same table.

(*ii*) *Theoretical results*

The results of Franck-Condon factors derived from Hutchisson's and Manneback's methods are entered in Table II.

TABLE II

Franck-Condon factors
BeO ($B \rightarrow X$) *system*

Band v', v''	Hutchisson	Manneback	Band v', v''	Hutchisson	Manneback
0, 0	0·886	0·886	2, 1	0·204	0·204
0, 1	0·102	0·102	2, 2	0·518	0·518
0, 2	0·011	0·011	2, 3	0·216	0·216
1, 0	0·111	0·111	2, 4	0·050	0·050
1, 1	0·685	0·685	3, 2	0·280	0·280
1, 2	0·172	0·172	3, 3	0·383	0·383
1, 3	0·029	0·029	3, 4	0·239	0·239
			3, 5	0·073	0·073

As expected the values under both the treatments are identical and they should be, so on considerations advanced by Tawde, Patil and Savadatti (1959).

For comparing the theoretical predictions with experimental values, the bands of each v''-progression are considered separately, since $N_{v'}$ populations are said to be constant for the group, and hence we should expect the two to vary relatively in the same proportion. The lowest band of each v''-progression is made to take the value unity for experimental I/ν^4 and similarly $P_{v'v''} = 1$ for theoretical transition probability. The results of other bands of the various v''-progressions are expressed on this basis. These values along with the ratio

$$\beta = \frac{\text{experimental } \dfrac{I}{\nu^4}}{P_{v'v''}}$$ are given in Table III.

If the theoretical predictions were to approximate to experimental data we would have expected the ratio β to be either unity or in the close neighbourhood of unity. But, that is not so. The ratio on the whole tends to depart widely with increasing v'' (*vide* Table III). The departure seems to be a

TABLE III

v''	Expt. I/ν^4	$P_{\bullet\bullet}'''$ (Manneback or Hutchisson)	$P_{\bullet\bullet}'''$ Pillow	$P_{\bullet\bullet}'''$ Bates	β_{SH} Manneback or Hutchisson	β Pillow	β Bates
			$v' = 0$				
0	1·000	1·000	1·000	1·000	1·00	1·00	1·00
1	0·235	0·115	0·066	0·115	2·04	3·56	2·04
2	0·009	0·012	0·005	0·004	0·75	1·80	2·25
			$v' = 1$				
0	1·000	1·000	1·000	1·000	1·00	1·00	1·00
1	20·730	6·171	6·229	7·120	3·36	3·33	2·91
2	10·454	1·550	0·898	1·780	6·74	11·64	5·87
3	0·493	0·261	0·068	0·100	1·89	7·25	4·93
			$v' = 2$				
1	1·000	1·000	1·000	1·000	1·00	1·00	1·00
2	11·813	2·539	2·823	3·476	4·65	4·18	3·40
3	8·097	1·059	0·790	1·404	7·65	10·25	5·77
4	0·444	0·245	0·006	0·102	1·81	74·00	4·35
			$v' = 3$				
2	1·000	1·000	1·000	1·000	1·00	1·00	1·00
3	7·784	1·368	1·346	2·309	5·69	5·78	3·37
4	7·550	0·854	0·710	1·319	8·84	10·63	5·72
5	0·793	0·261	0·035	0·111	3·04	22·66	7·14

consequence of the approximation taken, *viz.*, the simple harmonic character of the wave function. Actually, such an assumption is far from realisation in electronic bands where departure from parabolic curve towards anharmonic condition sets in after the first few vibrational levels. In considering, therefore, the verification of the theoretical predictions with experimental data, mechanical anharmonicity of the wave function would have to be taken into account. Further, the assumption, made in the two theories that the electronic transition moment is constant over the entire extent of internuclear separation, may not really hold. In order to have a systematic check on the results by inclusion of both of these factors, we shall first attempt to see if introduction of mechanical anharmonicity alone brings about improvement. For this we consider results from the method of Pillow (1951) and of Bates (1949).

(*a*) *Pillow's method.*—The values of transition probabilities obtained by this method are entered in Table IV. They are converted to the form of ratio β as in Manneback's method for comparison with experimental data and entered in last two columns of Table III.

TABLE IV

Transition probabilities (Pillow's New Distortion Process)
BeO ($B \rightarrow X$) system

v'' \ v'	0	1	2	3	4	5
0	0·888	0·059	0·004	..	..	..
1	0·118	0·735	0·106	0·008	..	..
2	..	0·181	0·511	0·143	0·001	..
3	..	..	0·286	0·385	0·203	0·010

We find from the values of β (Pillow) that there is still a large gap between theory and experiment although it appears relatively reduced in comparison to results from simple harmonic considerations. It is evident that the departure of theory from experiment increases with higher quanta. This aspect has been the subject of some discussion by Ta-You-Wu (1952). According to him, the wave functions obtained by distortion process have the same amplitude near both the turning points and consequently the error introduced on this account increases with vibrational quantum numbers. He has also

pointed out that there is a lack of orthogonality in the wave functions obtained by distortion process for the various states of anharmonic oscillator. This is also likely to introduce some error in relative transition probability. In our comparative results, the departure noticed may be a consequence of the above considerations, acting alone or in conjunction with the assumed constancy of R_e with r.

(*b*) *Bates' method.*—The resulting values of transition probabilities derived by this method with the use of Morse wave function (Bates, 1949) are entered in Table V. A check on these calculations was provided by the

TABLE V

Transition probabilities—Bates' method

BeO ($B \rightarrow X$) *system*

v' \ v''	0	1	2	3	4	5
0	0·893 (0·897)	0·103 (0·103)	0·004	..	..	..
1	0·100 (0·099)	0·712 (0·718)	0·178 ..	0·010	..	..
2	..	0·166 (0·164)	0·577	0·233	0·017	..
3	..	..	0·207	0·478	0·273	0·023

Note.— First row: Numerical integration (Morse).
Second row: Graphical integration (Lagerqvist, 1948).

values of a few bands available from the work on the verification of the absence of (3, 0) band in the system by Lagerqvist (1948). These values are given in parenthesis in Table V. It is obvious from the magnitude of β (Bates) (Table III) that there is an improvement of results over Pillow's method. However, on absolute considerations there is still an appreciable gap between the theoretical and experimental sets of results, as the latter values continue to be many times the theoretical ones, in some bands. This may mean that the factor of mechanical anharmonicity alone of the wave functions may not be enough in the theoretical concepts. The exact variation

of electronic transition moment R_e, which has been neglected in the theory by considering it as a constant, may have to be taken into account along with anharmonicity. Shuler (1950, 1952) has shown it to be effective in the case of bands of OH ($A\,^2\Sigma \rightarrow X\,^2\Sigma$) system. Hence we shall see how our results on BeO system shape under the contribution of R_e as a function of r, in addition to anharmonicity of the wave functions.

Methods Involving Variation of Electronic Transition Moment

(*a*) *Shuler's procedure.*—The method of Shuler as applied by him to OH ($A \rightarrow X$) system has been extended to the BeO system. For the evaluation of the integral

$$| M_{v'v''} | = \int \psi_{v'}(r)\, \psi_{v''}(r)\, R_e\, dr. \qquad \text{(i)}$$

Shuler has assumed a linear variation of R_e as follows:

$$R_e = c(1 + \rho r) \qquad \text{(ii)}$$

where ρ is the expansion coefficient. For a pair of bands, arising from the same initial level, the ratio of quantities I/ν^4 associated with them, will be the ratio (P_{jk}/P_{ji}) of the transition probabilities of these bands. Using this ratio and equations (i) and (ii), ρ can be evaluated with the knowledge of the integrals $\int \psi_{v'}(r)\, \psi_{v''}(r)\, dr$ and $\int \psi_{v'}(r)\, \psi_{v''}(r)\, r dr$.

From the observed integrated intensities of bands in BeO ($B \rightarrow X$) system, the following ratios are obtained:

$$\frac{|M_{00}|^2}{|M_{01}|^2} = 4{\cdot}25_3; \quad \frac{|M_{11}|^2}{|M_{12}|^2} = 1{\cdot}98_3; \quad \text{and} \quad \frac{|M_{23}|^2}{|M_{21}|^2} = 8{\cdot}09_7.$$

The values of integrals $\int \psi_{v'}(r)\, \psi_{v''}(r)\, dr$ and $\int \psi_{v'}(r)\, \psi_{v''}(r)\, r dr$ are available from the results of Bates' method. With the help of these integrals and the above ratios for three pairs, ρ has been evaluated. Since ρ appears as a quadratic in the equation, it has double roots. Out of the two roots, $\rho_{average} = -0{\cdot}982_2$ and $\rho'_{average} = -0{\cdot}724_2$, the physically meaningful root $\rho_{av} = -0{\cdot}982_2$ is chosen. Hence the electronic transition moment variation is given by

$$R_e = c(-1 + 0{\cdot}982_2\, r)$$

where c is a constant. This expression therefore governs the variation of R_e with r for BeO ($B \rightarrow X$) system. The values of $P_{v'v''}/P_{00}$ obtained from Bates' method have been corrected in terms of the above variation of electronic transition moment and are recorded in Table VI.

TABLE VI

Corrected $P_{v'v''}/P_{00}$ for BeO system

v' \ v''	0	1	2	3	4	5
0	1·000	0·234	0·016	..	..	..
1	0·042	0·853	0·431	0·042	..	..
2	..	0·073	0·741	0·601	0·075	..
3	..	..	0·096	0·658	0·753	0·111

(*b*) *Method of r-centroids.*—From the concepts of *r*-centroids first developed by Nicholls and Jarmain (1956), the following expression involving $R_e(r)$ may be evolved:

$$\left(\frac{I_{v'v''}}{q_{v'v''}\,\nu^4_{v'v''}}\right)^{\frac{1}{2}} = (KN_{v'})^{\frac{1}{2}}\, R_e(\bar{r}_{v'v''})$$

where

$I_{v'v''}$ = measured integrated intensity,

$q_{v'v''}$ = Franck-Condon factor

and

$\bar{r}_{v'v''}$ = *r*-centroid.

Nicholls (1956) has used this to determine variation of $R_e(r)$ with r for each v''-progression. For this purpose, the values of $q_{v'v''}$ and $\bar{r}_{v'v''}$ need to be known. The former of these are available from Table V above under Bates' method. For the values of the latter, *viz.*, $\bar{r}_{v'v''}$ computations are made by procedures which are given in a separate paper under publication elsewhere. These two quantities for BeO bands as well as $I_{v'v''}/\nu^4_{v'v''}$ data are entered in Table VII. A graphical plot of the quantity $(I_{v'v''}/\nu^4_{v'v''}\, q_{v'v''})^{\frac{1}{2}}$ is made against $\bar{r}_{v'v''}$. By adopting the rescaling procedure of Turner and Nicholls (1954) segments are placed on the same ordinate scale. The plot of $R_e(\bar{r}_{v'v''})$ against $\bar{r}_{v'v''}$ is made. By applying the least square technique, the best fit for the straight line is found to be satisfied by the relation of the standard form:

$$R_e(r) = c(-1 + 0{\cdot}990_6\, r),$$

TABLE VII

Band v', v''	$r_{v'v''}$ (Numerical integration, Morse)	$q_{v'v''}$ (Numerical integration, Morse)	$\frac{I_{v'v''}}{\nu^4_{v'v''}}$	$\frac{P_{v'v''}}{P_{00}}$
0, 0	1·352	0·893	49·21	1·000
0, 1	1·492	0·103	11·57	0·229
0, 2	1·642	0·004	0·45	0·015
1, 0	1·222	0·100	1·52	0·043
1, 1	1·363	0·712	31·51	0·849
1, 2	1·508	0·178	15·89	0·422
1, 3	1·662	0·010	0·75	0·041
2, 1	1·227	0·166	1·44	0·075
2, 2	1·375	0·577	17·01	0·736
2, 3	1·524	0·233	11·66	0·589
2, 4	1·685	0·017	0·64	0·074
3, 2	1·232	0·207	1·11	0·098
3, 3	1·388	0·478	8·64	0·654
3, 4	1·541	0·273	8·38	0·736
3, 5	1·708	0·023	0·88	0·107

This equation represents therefore the behaviour of the variation of electronic transition moment $R_e(r)$ with r, the internuclear distance for the bands of BeO ($B\,^1\Sigma \rightarrow X\,^1\Sigma$) system over the range $1{\cdot}222\,\text{Å} > r > 1{\cdot}708\,\text{Å}$. A set of smoothed $R_e(\bar{r}_{v'v''})$ has been obtained from the above equation. These values are multiplied by appropriate Franck-Condon factors, $q_{v'v''}$, to correct the transition probabilities obtained with Bates' method. Thus the final corrected or smoothed set of $P_{v'v''}/P_{00}$ values are evolved for the system which are entered in column 5 of Table VII.

For comparing the transition probabilities obtained independently from Shuler's and r-centroid methods with the experimental data, Table VIII has been compiled.

Discussion

The expression found for $R_e(r)$ by the two independent approaches are:

Shuler's method: $R_e(r) = c(-1 + 0{\cdot}982_2\, r)$

r-centroid method: $R_e(r) = c(-1 + 0{\cdot}990_5\, r)$

Both the expressions are uniform giving nearly the same expansion coefficient, ρ for r. Of the two methods, the *r*-centroid method uses larger number of measured intensities for the derivation of the relation, while that of Shuler makes use of only a few measured intensities. The former, *viz.*, the *r*-centroid method is therefore considered to be a better representative and hence preferred to the latter, *i.e.*, Shuler's method. Both the methods depend on the experimental intensity data and are thus quasi-theoretical. The comparison between the experimental I/ν^4 and corrected or smoothed $P_{v'v''}$ has been made here, only to ascertain whether the linear trend of the variation of $R_e(r)$ is justified. In the last two columns of Table VIII, the ratio β is almost unity for bands in all the sequences except $\Delta v = -2$. This indicates that the corrected or sooothed transition probabilities by both the methods are in general agreement with experimental measures. The large deviations in the bands of $\Delta v = -2$ sequence are attributed to want of precision (1) in experimental intensities due to comparative feebleness of these bands and (2) in theoretical measures due to low values of overlap integrals arising from the large cancellation of positive and negative contributions of the products of the wave functions of comparable magnitude, the partial neglect of vibration rotation interaction and, to some extent, the limited applicability of Morse potential. For these reasons, the evaluation of relation of $R_e(r)$ with r is made independent of these bands by excluding them in the graphical plot.

The relatively much closer agreement between these results of quasi-theoretical concepts and experimental observations on the bands of BeO ($B \rightarrow X$) system confirm the conclusion of Shuler (1950, 1952) that the variation of $R_e(r)$ with r is a great contributing factor, besides the anharmonicity of the wave functions in theoretical considerations of transition probabilities. The results indicate that the assumption generally made that the electronic transition moment is constant along r is therefore not justified.

TABLE VIII

v''	Experimental I/ν^4	$P'_{v'v''}$ (Shuler)	$P'_{v'v''}$ (r-centroid)	$\beta = \frac{\text{Expt. } (I/\nu^4)}{P'_{v'v''}}$ (Shuler)	β (r-centroid)
			$v' = 0$		
0	1·000	1·000	1·000	1·00	1·00
1	0·235	0·234	0·229	1·00	1·03
2	0·009	0·016	0·015	0·56	0·60
			$v' = 1$		
0	1·000	1·000	1·000	1·00	1·00
1	20·730	20·310	19·744	1·02	1·05
2	10·454	10·262	9·814	1·02	1·07
3	0·493	1·000	0·953	0·49	0·52
			$v' = 2$		
1	1·000	1·000	1·000	1·00	1·00
2	11·813	10·151	9·813	1·16	1·20
3	8·097	8·233	7·853	0·98	1·03
4	0·444	1·027	0·987	0·43	0·45
			$v' = 3$		
2	1·000	1·000	1·000	1·00	1·00
3	7·784	6·854	6·673	1·14	1·17
4	7·550	7·844	7·510	0·96	1·01
5	0·793	1·156	1·092	0·69	0·73

5. SUMMARY

Accurate integrated intensity data of the bands of BeO ($B\,^1\Sigma \rightarrow X\,^1\Sigma$) system has been obtained experimentally by the technique of photographic photometry. With the use of Franck-Condon factors and r-centroids for

the bands available from the work of the authors reported in papers elsewhere, the relation of electronic transition moment R_e with internuclear separation r, has been evolved. The vibrational transition probabilities have been corrected for the resulting variation of R_e with r. These corrected values have been examined in relation to those under assumptions of constancy of R_e in conjunction with (i) mechanical anharmonicity and also (ii) mechanical harmonicity.

6. Acknowledgment

One of the authors (N. S. M.) is grateful to the Ministry of Education, Government of India, for the award of a Senior Research Training Scholarship, which enabled this investigation to be carried out.

7. References

Bates, D. R. .. *Proc. Roy. Soc.*, 1949, **196 A**, 217.

Davis, D. N. .. *Ap. J.*, 1947, **106**, 28.

Dunham, J. L. .. *Phys. Rev.*, 1930, **36**, 1553.

Elliott, A. .. *Proc. Phys. Soc.* (*Lond.*), 1933, **45**, 627.

—— and Cameron, W. H. B. *Ibid.*, 1934, **46**, 801.

Gaydon, A. G. and Pearse, R. W. B. *Ibid.*, 1939, **173 A**, 37.

Herzberg, G. .. *Spectra of Diatomic Molecules*, 2nd Edition, D. Van. Nostrand Co., New York, 1950, p. 509.

Hutchisson, E. .. *Phys. Rev.*, 1930, **36**, 410.

Johnson, R. C. and Dunstan, E. G. *Phil. Mag.*, 1933, **16**, 472.

Lagerqvist, A. .. *Dissertation*, Stockholm, 1948, p. 27.

Manneback, C. .. *Physica*, 1951, **17**, 1001.

Nicholls, R. W. .. *Proc. Phys. Soc.* (*Lond.*), 1956, **69 A**, 741.

——— and Jarmain, W. R. .. *Ibid.*, 1956, **69 A**, 253.

Pillow, M. E. .. *Ibid.*, 1951, **64 A**, 772.

Shuler, K. E. .. *J. Chem. Phys.*, 1950, **18**, 1221.

——— .. *Proc. Phys. Soc.* (*Lond.*), 1952, **65 A**, 12.

Tawde, N. R. and Patankar, V. S. *Ibid.*, 1943, **55**, 396.

——— and Hussain, A. G. .. *Bom. Uni. Jour.*, 1949, **17**, 12.

———, Patil, B. S. Sreedhara Murthy, N. and Katti, M. R. *Physica*, 1957, **23**, 154.

———, and Patil, B. S. *Bull. Soc. Royale, Sciences Liege Belgique*, 1959, **5-6**, 150.

———, Savadatti, M. I. and Sreedhara Murthy, N. *Physica*, 1959, **25**, 610.

Turner, R. G. and Nicholls, R. W. *Canad. J. Phys.*, 1954, **32**, 475.

Wu-Ta-You .. *Proc. Phys. Soc.* (*Lond.*), 1952, **65 A**, 965.

296-60 Printed at the Bangalore Press, Bangalore City, by T. K. Balakrishnan, Superintendent, and Published by The Indian Academy of Sciences, Bangalore.

NOTICE TO AUTHORS

Scientific papers intended for publication in the *Proceedings of the Indian Academy of Sciences* can be accepted only when they are communicated by a Fellow of the Academy whose duty shall be to satisfy himself that such communications are fit to be read at the Meeting of the Academy and published in its *Proceedings*.

Papers should not ordinarily exceed fifty pages of foolscap. MSS. should be either typewritten or written in legible hand on one side of the paper. All papers should be carefully revised by the authors and should be absolutely in final form for printing. Position for text-figures should be indicated. Each paper shall conclude with a critical summary not exceeding 350 words.

Drawings, diagrams or other illustrations should be made on larger scale (preferably) twice the size than the ones in which they are intended to appear. They should be done in Indian ink on bristol board with lettering in pencil. Scale of magnification of camera lucida tracings should be indicated by the side of drawings. In certain special cases arrangements will also be made for monochrome lithographic and other colour plates. Reduction of illustrations desired should be indicated in pencil. Appropriate legends should accompany all drawings. Names of authors are to be marked in pencil on the left-hand corner of drawing sheets. Photomicrographs should be securely mounted with colourless paste.

All tables, quotations and footnotes which will be set hereafter (beginning from Vol. I, No. 2) in types smaller than the text, should be typewritten on separate sheets and placed with the text in proper sequence. Footnotes should be numbered in Arabic numerals.

References to literature in the text should be given, whenever possible, in chronological order, only the names of authors and years of publication, in brackets, being given. They should be cited in full after the summary, the authors' names following in alphabetical order. Thus,

Name or Names of author; Name of Journal (abbreviation) with a single underline; Year of publication; Number of Volume with a double underline, and lastly page. The following would be a useful illustration:—

Bergmann and Stather . . . . . Z. Physiol. Chem., 1926, 152, 189.

Two copies of slip-proof and wherever possible, a page proof for final revision will be sent to authors. All corrections are best made on the slip-proof which should be transmitted to the Office of the Academy. All proof corrections involve heavy expenses which would be negligible if the papers are carefully revised by the authors before submission.

Fifty free reprints including plates and with cover will be supplied for each paper. Additional copies can be supplied at cost on previous intimation.

Blocks appearing in the *Proceedings* will be available for purchase by their respective authors. Orders for the same should be sent along with the corrected proofs and in any case not later than one month after the date of publication of the paper. The price charged would be 75% of the actual cost of the blocks *plus* freight and despatching charges. If the blocks are reproduced in other journals or publications, due acknowledgment should be made in them to the *Proceedings*.

The original drawings and plates of blocks appearing in the *Proceedings* will be returned to such of the authors as may require them provided the cost of despatching such originals is borne by them.

CONTENTS

PAGE

Potentiometric Studies on the Dissociation of Gallic Acid . . . . . N. A. Ramaiah and R. K. Chaturvedi 177

Study of Solar Flares Using Cosmic Radio Noise on 25 Mc./s. at Ahmedabad (23° 02′ N., 72° 38′ E.). . . . . R. V. Bhonsle 189

Ore-Microscopic Studies of the Manganese Ore-Minerals of Old M.P. II. Satak, Beldongri, Lohdongri and Kachurwahi, Nagpur District. . . . . S. P. Deshpande 202

Electronic Transition Moment Variation in ($B^1\Sigma \rightarrow X^1\Sigma$) Bands of BeO . . . . . N. R. Tawde and N. Sreedhara Murthy 219